

Tropical Gradient Descent

Roan Talbut^{1,†} and Anthea Monod¹

1 Department of Mathematics, Imperial College London, UK

† Corresponding e-mail: r.talbut21@imperial.ac.uk

Abstract

We propose a gradient descent method for solving optimization problems arising in settings of tropical geometry—a variant of algebraic geometry that has attracted growing interest in applications such as computational biology, economics, and computer science. Our approach takes advantage of the polyhedral and combinatorial structures arising in tropical geometry to propose a versatile method for approximating local minima in tropical statistical optimization problems—a rapidly growing body of work in recent years. Theoretical results establish global solvability for 1-sample problems and a convergence rate matching classical gradient descent. Numerical experiments demonstrate the method’s superior performance compared to classical gradient descent for tropical optimization problems which exhibit tropical convexity but not classical convexity. We also demonstrate the seamless integration of tropical descent into advanced optimization methods, such as Adam, offering improved overall accuracy.

Keywords: tropical quasi-convexity; tropical projective torus; gradient descent; phylogenetics.

1 Introduction

Where algebraic geometry studies geometric properties of solution sets of systems of multivariate polynomials, *tropical geometry* restricts to the case of polynomials defined by linearizing operations, where the “sum” of two elements is their maximum and the “product” of two elements is their sum. Evaluating polynomials with these operations results in piecewise linear functions. Tropical geometry is a relatively young field of pure mathematics established in the 1990s (with roots dating back further) and has recently become an area of active interest in computational and applied mathematics for its relevance to the statistical analyses of phylogenetic trees (Monod *et al.*, 2018), the problem of dynamic programming in computer science (Maclagan & Sturmfels, 2015), and in mechanism design for two-player games in game theory (Lin & Tran, 2019). Following the identification of the tropical Grassmannian and the space of phylogenetic trees (Speyer & Sturmfels, 2004) in particular, there has been a surge of research (Barnhill *et al.*, 2024; Lin & Yoshida, 2018; Comănesci & Joswig, 2024; Monod *et al.*, 2018) which necessitates the development of new computational techniques for optimization in tropical geometric settings.

Training machine learning models and many computational tasks in statistics entail solving optimization problems; this paper is motivated by statistical optimization problems in tropical geometric settings. Early research in tropical statistics focused on optimization problems such as the identification of Fermat–Weber points which, due to the piecewise linear nature of tropical geometry, can be re-framed as a linear program (Comănesci & Joswig, 2024; Lin & Yoshida, 2018). Unfortunately, the complexity of these linear programs often scales poorly with the size of our dataset, so gradient methods are more commonly implemented in practice (Sabot *et al.*, 2024; Barnhill *et al.*, 2024). More recently—following the identification of ReLU neural networks and tropical rational functions (Zhang *et al.*, 2018)—more sophisticated neural network optimization problems are being studied in the tropical setting (Pasque *et al.*, 2024; Yoshida *et al.*, 2024), which necessitates the use of gradient methods for optimization in the tropical setting. In this paper, we address the natural question—given the need for gradient methods in tropical data science, how can we tailor classical gradient methods to the tropical setting? We provide a foundational tropical gradient descent framework to solve the optimization problems which arise in the computation of a wide range of tropical statistics, an area of active interest in applied tropical geometry.

The remainder of this paper is organized as follows. The following section contains the necessary foundations of tropical geometry, an introduction to tropical location problems (Comănesci, 2024), and an overview

of the statistical optimization tasks studied in this paper. [Section 3](#) contains the theoretical contributions of this paper; we formulate steepest descent with respect to the tropical norm and present the theoretical guarantees for tropical descent, most notably its convergence for a wide class of tropically quasi-convex functions and a convergence rate of $O(1/\sqrt{m})$. In [Section 4](#), we perform a comprehensive numerical study of our proposed tropical descent method and its performance in the statistical optimization problems of interest. We conclude with a discussion of possible future work on tropical gradient methods in [Section 5](#).

2 Background and Preliminaries

In this section, we present a summary of tropical geometry and the statistical optimization problems which we study in the tropical setting.

2.1 Tropical Geometry

We begin by reviewing the algebraic and geometric structure of the tropical projective torus, the state space for phylogenetic data and the domain of our tropical statistical optimization problems.

Definition 1 (Tropical Algebra). The *tropical algebra* is the semiring $\overline{\mathbb{R}} = \mathbb{R} \cup \{-\infty\}$ with the addition and multiplication operators—tropical addition and tropical multiplication, respectively—given by

$$a \boxplus b = \max\{a, b\}, \quad a \odot b = a + b.$$

The additive identity is $-\infty$ and the multiplicative identity is 0 . Tropical subtraction is not defined; tropical division is given by classical subtraction.

The tropical algebra defined above is sometimes referred to as the *max-plus algebra*; we can define the min-plus algebra analogously, taking $\min\{a, b\} =: a \oplus b$ as the additive operation on $\mathbb{R} \cup \{\infty\}$. These are algebraically equivalent under negation. Unless specified, we use the max-plus convention as this is better suited for phylogenetic statistics on the tropical projective torus (Speyer & Sturmfels, 2004).

Definition 2 (Tropical Projective Torus). The $N - 1$ -dimensional *tropical projective torus* is a quotient space constructed by endowing \mathbb{R}^N with the equivalence relation

$$\mathbf{x} \sim \mathbf{y} \Leftrightarrow \exists a \in \mathbb{R} : \mathbf{x} = a \odot \mathbf{y}; \tag{1}$$

it is denoted by $\mathbb{R}^N / \mathbb{R}\mathbf{1}$. The generalized Hilbert projective metric, also referred to as the *tropical metric*, is given by

$$d_{\text{tr}}(\mathbf{x}, \mathbf{y}) = \max_i (x_i - y_i) - \min_i (x_i - y_i) = \max_{i,j} (x_i - y_i - x_j + y_j).$$

This metric is induced by the tropical norm, which is given by

$$\|\mathbf{x}\|_{\text{tr}} = \max_i x_i - \min_i x_i.$$

Remark 3. While a single point in the tropical projective torus is given by some ray $\mathbf{x} + \mathbb{R}\mathbf{1}$, we note that there is a unique representative of this equivalence class whose coordinates sum to zero. In taking such representatives, we can identify the tropical projective torus $\mathbb{R}^N / \mathbb{R}\mathbf{1}$ and the hyperplane $\mathcal{H} = \{\mathbf{x} \in \mathbb{R}^N : \sum x_i = 0\}$. Throughout this paper, we use this homeomorphism to visualize the tropical projective torus (e.g., [Figures 1 and 2](#)).

The tropical projective torus is the ambient space containing the tropical Grassmannian, which is equivalent to the space of phylogenetic trees (Speyer & Sturmfels, 2004). This has sparked the study of tropical data science, formalizing statistical techniques which respect the tropical geometry of the state space (Monod *et al.*, 2018; Yoshida, 2022).

The generalized Hilbert projective metric defined above is widely accepted and preferred for the development of geometric statistical tools on the tropical projective torus (Yoshida, 2022). However, recent work has shown theoretical advantages to the use of an asymmetric metric (Comănesci & Joswig, 2024).

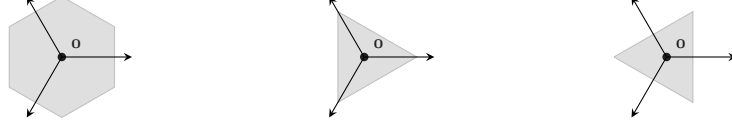


Figure 1: The d_{tr} , $d_{\Delta_{\min}}$ and $d_{\Delta_{\max}}$ tropical unit balls in $\mathbb{R}^3/\mathbb{R}\mathbf{1} \cong \mathcal{H} = \{\sum x_i = 0\}$. The solid lines show coordinate directions.

Definition 4 (Tropical Asymmetric Distance). The *tropical asymmetric distances* on $\mathbb{R}^N/\mathbb{R}\mathbf{1}$ are given by

$$d_{\Delta_{\min}}(\mathbf{a}, \mathbf{b}) := \sum_i (b_i - a_i) - N \min_j (b_j - a_j),$$

$$d_{\Delta_{\max}}(\mathbf{a}, \mathbf{b}) := N \max_j (b_j - a_j) - \sum_i (b_i - a_i).$$

Remark 5. The asymmetric distances act as an ℓ_1 norm on the tropical projective torus, while the symmetric metric d_{tr} acts as an ℓ_∞ norm. We note that $Nd_{\text{tr}} = d_{\Delta_{\min}} + d_{\Delta_{\max}}$. Figure 1 shows the balls for each tropical metric of interest.

We now define the primary geometric objects of interest in the tropical projective torus; hyperplanes, lines, and convex hulls. We use the max-convention for these definitions, though we note each has a min-convention equivalent.

Definition 6 (Tropical Hyperplane). The *tropical hyperplane* $\mathcal{H}_{\mathbf{a}}$ defined by the linear form $a_1 \odot x_1 \boxplus \dots \boxplus a_N \odot x_N$ is given by

$$\mathcal{H}_{\mathbf{a}} = \{\mathbf{x} \in \mathbb{R}^N/\mathbb{R}\mathbf{1} : \exists i \neq j \text{ s.t. } a_i + x_i = a_j + x_j = \max_k (a_k + x_k)\}.$$

Definition 7 (Tropical Line Segment). For any two points $\mathbf{a}, \mathbf{b} \in \mathbb{R}^N/\mathbb{R}\mathbf{1}$, the *tropical line segment* between \mathbf{a} and \mathbf{b} is the set

$$\gamma_{\mathbf{ab}} = \{\alpha \odot \mathbf{a} \boxplus \beta \odot \mathbf{b} \mid \alpha, \beta \in \mathbb{R}\}$$

with tropical addition taken coordinate-wise.

Tropical line segments define a unique geodesic path between any two points, but general geodesics are not uniquely defined on the tropical projective torus.

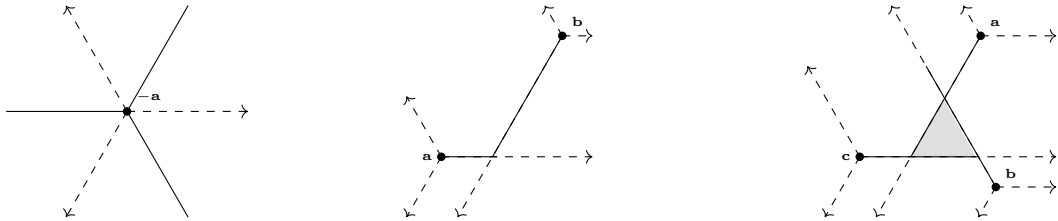


Figure 2: A tropical hyperplane, tropical line segment and tropical convex hull in $\mathbb{R}^3/\mathbb{R}\mathbf{1} \cong \mathcal{H} = \{\mathbf{x} : \sum x_i = 0\}$. The dashed lines show coordinate directions.

Definition 8 (Tropical Convex Hull (Develin & Sturmfels, 2004)). A set $S \subset \mathbb{R}^N/\mathbb{R}\mathbf{1}$ is *max-tropically convex* if it contains $\alpha \odot \mathbf{x} \boxplus \beta \odot \mathbf{y}$ for all $\mathbf{x}, \mathbf{y} \in S$ and $\alpha, \beta \in \mathbb{R}$. For a finite subset $X = \{\mathbf{x}_1, \dots, \mathbf{x}_K\} \subset \mathbb{R}^N/\mathbb{R}\mathbf{1}$, the *max-plus tropical convex hull* of X is the set of all max-tropical linear combinations of points in X ,

$$\text{tconv}_{\max}(X) := \{\alpha_1 \odot \mathbf{x}_1 \boxplus \dots \boxplus \alpha_K \odot \mathbf{x}_K \mid \alpha_1, \dots, \alpha_K \in \mathbb{R}\}.$$

Similarly, the *min-tropical convex hull* of X , $\text{tconv}_{\min}(X)$, is the set of all min-tropical linear combinations of points in X .

A study of tropically convex functions requires an understanding of both max-tropical and min-tropical convexity, as we will see in our following consideration of tropical location problems.

2.2 Tropical Location Problems

Tropical location problems are a new avenue of research, motivated by the optimization of statistical loss functions; they involve the minimization over some dataset of some loss function which heuristically increases with distance from some kernel. Here we outline the relevant definitions of tropical location problems and their theoretical behavior as presented by Comănesci (2024). We introduce the problem of tropical linear regression (Akian *et al.*, 2023) as motivation.

2.2.1 Motivating Example

The problem of tropical linear regression looks to find the best-fit tropical hyperplane which minimizes the maximal distance to a set of data points. While this is an inherently statistical optimization problem, it has recently been proven to be polynomial-time equivalent to solving mean payoff games (Akian *et al.*, 2023).

A tropical hyperplane is uniquely defined by a cone point $\mathbf{t} \in \mathbb{R}^N/\mathbb{R}\mathbf{1}$, allowing us to formulate the best-fit tropical hyperplane as an optimization problem over $\mathbf{t} \in \mathbb{R}^N/\mathbb{R}\mathbf{1}$.

Definition 9 (Tropical Linear Regression (Akian *et al.*, 2023)). Let $X = \{\mathbf{x}_1, \dots, \mathbf{x}_K\} \subset \mathbb{R}^N/\mathbb{R}\mathbf{1}$ be our dataset. The *tropical linear regression problem* finds the vertex $\mathbf{t} \in \mathbb{R}^N/\mathbb{R}\mathbf{1}$ of the best-fit hyperplane:

$$\min_{\mathbf{t} \in \mathbb{R}^N/\mathbb{R}\mathbf{1}} f(\mathbf{t}) = \max_{k \leq K} d_{\text{tr}}(\mathbf{x}_k, \mathcal{H}_{\mathbf{t}}) = \max_{k \leq K} (\max_i (\mathbf{x}_k - \mathbf{t})_i - 2\text{ndmax}_i (\mathbf{x}_k - \mathbf{t})_i)$$

where $2\text{ndmax}_i y_i$ denotes some y_i such that $\exists j \neq i$ such that $\forall k \neq i, j: y_j \geq y_i \geq y_k$.

This expression for the tropical distance between \mathbf{x} and $\mathcal{H}_{\mathbf{t}}$ was first stated by Gärtner & Jaggi (2006), and has been frequently used in the ongoing study of tropical support vector machines (Yoshida *et al.*, 2023; Tang *et al.*, 2024).

In Figure 3, we see a heatmap of this objective function over the tropical projective plane for a sample of size 3. We see immediately that the objective is not convex. The linear regression objective has sparse gradient almost everywhere, which produces valleys. These properties are considered unfavorable extreme cases for gradient methods, but are particularly common in tropical optimization problems. While the tropical linear regression problem is not convex, it is quasi-convex along tropical line segments; that is, its sub-level sets are tropically convex.

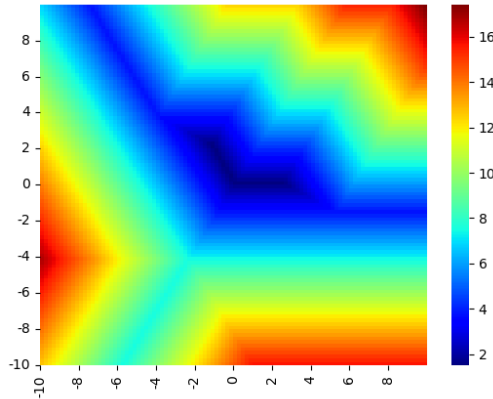


Figure 3: A heat map of a 3-sample linear regression objective on $\mathbb{R}^3/\mathbb{R}\mathbf{1} \cong \mathcal{H} = \{\mathbf{x} : \sum x_i = 0\}$.

2.2.2 Quasi-Convexity of Tropical Functions

In formalizing tropical location problems, the work of Comănesci (2024) first considers functions which increase along tropical geodesics from a kernel \mathbf{v} ; that is, for any point \mathbf{t} on a geodesic from \mathbf{v} to \mathbf{w} , we have that $f(\mathbf{t}) \leq f(\mathbf{w})$. This property is equivalent to star-convexity of sub-level sets. To formally state this, we define (oriented) geodesic segments and Δ_{\min} -star convexity of sets.

Definition 10 (Oriented Geodesic Segment). The (*oriented*) *geodesic segment* between $\mathbf{a}, \mathbf{b} \in \mathbb{R}^N/\mathbb{R}\mathbf{1}$, is given by $[\mathbf{a}, \mathbf{b}]_{\Delta_{\min}} := \{\mathbf{x} \in \mathbb{R}^N/\mathbb{R}\mathbf{1} : d_{\Delta_{\min}}(\mathbf{a}, \mathbf{x}) + d_{\Delta_{\min}}(\mathbf{x}, \mathbf{b}) = d_{\Delta_{\min}}(\mathbf{a}, \mathbf{b})\}$.

The oriented geodesic segment is the union of all geodesics from \mathbf{a} to \mathbf{b} with respect to $d_{\Delta_{\min}}$.

Definition 11 (Δ_{\min} -Star Convex Set). A set $S \subseteq \mathbb{R}^N/\mathbb{R}\mathbf{1}$ is a Δ_{\min} -*star-convex* set with kernel \mathbf{v} if, for every $\mathbf{w} \in S$, we have $[\mathbf{v}, \mathbf{w}]_{\Delta_{\min}} \subseteq S$.

Using the above definitions, we can characterize a loss function which is increasing along tropical geodesics as a function with Δ_{\min} -star-convex sub-level sets. The following definition gives a closed form expression for such functions, while [Theorem 13](#) proves their equivalence.

Definition 12 (Δ_{\min} -Star-Quasi-Convex Functions (Comăneci, 2024)). A function $f : \mathbb{R}^N/\mathbb{R}\mathbf{1} \rightarrow \mathbb{R}$ is Δ_{\min} -*star-quasi-convex* with kernel \mathbf{v} if $f(\mathbf{x}) = \hat{\gamma}(\mathbf{x} - \mathbf{v})$ for some $\gamma : \mathbb{R}_{\geq 0}^N \rightarrow \mathbb{R}$ which is increasing in every coordinate, where we define $\hat{\gamma}(\mathbf{x}) := \gamma(\mathbf{x} - (\min_i x_i)\mathbf{1})$.

Theorem 13 (Theorem 17 of Comăneci (2024)). *A continuous function $f : \mathbb{R}^N/\mathbb{R}\mathbf{1} \rightarrow \mathbb{R}$ is Δ_{\min} -star-quasi-convex with kernel \mathbf{v} if and only if all of its non-empty sub-level sets are Δ_{\min} -star convex with kernel \mathbf{v} .*

Remark 14. We can define Δ_{\max} -star-quasi-convex functions similarly, but we also note that a function $f(\mathbf{t})$ is a Δ_{\max} -star-quasi-convex function if and only if $f(-\mathbf{t})$ is a Δ_{\min} -star-quasi-convex function.

These Δ_{\min} -star-convex functions serve as a loss function with respect to a single data point. For example, the tropical metric d_{tr} is both Δ_{\min} and Δ_{\max} -star-quasi-convex. The distance to a hyperplane $d_{\text{tr}}(\mathbf{x}, \mathcal{H}_{\mathbf{t}})$ is Δ_{\max} -star-quasi-convex in \mathbf{x} , but Δ_{\min} -star-quasi-convex in \mathbf{t} .

As a final remark, we note that Δ_{\min} -star-quasi-convex functions are a special case of tropically quasi-convex functions by the following lemma. We limit our theoretical considerations to Δ_{\min} -star-quasi-convex functions to utilize their closed form expression given in [Theorem 12](#), however numerical experiments demonstrate strong performance of our methodology for more general tropical quasi-convex functions.

Proposition 15 (Proposition 8 of Comăneci (2024)). *Any Δ_{\min} -star-convex set is min-tropically convex. Hence, any Δ_{\min} -star-quasi-convex function is tropically quasi-convex in that it has tropically convex sub-level sets.*

2.2.3 Tropical Location Problems

The Δ_{\min} -star-convex functions defined above are generally a measure of closeness to the kernel \mathbf{v} , but in minimizing a statistical loss function we consider proximity to a sample of points. A *location problem* (Laporte *et al.*, 2019) measures the closeness to a sample rather than a single kernel.

Definition 16 (Min(/max)-Tropical Location Problem (Comăneci, 2024)). Consider a dataset $X = \{\mathbf{x}_1, \dots, \mathbf{x}_K\} \subset \mathbb{R}^N/\mathbb{R}\mathbf{1}$. For $k \leq K$, let h_k be a Δ_{\min} -star-quasi-convex function with kernel \mathbf{x}_k , and let $g : \mathbb{R}^K \rightarrow \mathbb{R}$ be increasing in every coordinate. A *min-tropical location problem* is the minimization of an objective function $f : \mathbb{R}^N/\mathbb{R}\mathbf{1} \rightarrow \mathbb{R}$ given by $f = g(h_1, \dots, h_K)$. A *max-tropical location problem* is defined similarly, where the h_k are Δ_{\max} -star-quasi-convex.

The main result of Comăneci (2024) is the following: tropical location problems contain a minimum in the tropical convex hull of its dataset X .

Theorem 17 (Theorem 20 of Comăneci (2024)). *Let f be the objective function of a min-tropical location problem. Then there is a minimum of f belonging to $\text{tconv}_{\max}(X)$. Conversely, max-tropical location problems have minima belonging to $\text{tconv}_{\min}(X)$.*

We can now revisit our motivating example ([Theorem 9](#)), showing that tropical linear regression is not just a min-tropical location problem, but also demonstrates tropical quasi-convexity in that it has tropically convex sub-level sets.

Proposition 18. *The tropical linear regression problem is a min-tropical location problem with tropically convex sub-level sets.*

Proof

$$\begin{aligned}
f(\mathbf{t}) &= \max_{k \leq K} (\max_i (\mathbf{x}_k - \mathbf{t})_i - 2 \text{ndmax}_i (\mathbf{x}_k - \mathbf{t})_i) \\
&= \max_{k \leq K} 2 \text{ndmin}_j (\max_i (x_{ki} - t_i) - x_{kj} + t_j) \\
&= \max_{k \leq K} 2 \text{ndmin}_j (t_j - x_{kj} - \min_i (t_i - x_{ki}))
\end{aligned}$$

This is a min-tropical location problem with:

$$\begin{aligned}
g(\mathbf{h}) &= \max_{k \leq K} h_k, \\
h_k(\mathbf{t}) &= \hat{\gamma}(\mathbf{t} - \mathbf{x}_k), \\
\gamma(\mathbf{t}) &= 2 \text{ndmin}_i t_i.
\end{aligned}$$

This g and γ are increasing in each coordinate and each h_k has kernel \mathbf{x}_k , satisfying the conditions for a min-tropical location problem.

As the h_k are Δ_{\min} -star-convex, their sub-level sets are min-tropically convex by [Theorem 15](#). This is preserved when taking a maximum over samples, so f also has min-tropically convex sub-level sets. \square

As mentioned in [Theorem 15](#), Δ_{\min} -star-quasi-convexity implies tropical quasi-convexity. However, the tropical linear regression problem is a case in which the reverse implication does not hold; in general, the linear regression loss function is not Δ_{\min} -star-quasi-convex.

2.3 Tropical Data Science

While young, the field of tropical data science is motivated by the crucial question of statistical learning from the increasing volume of phylogenetic tree data (Kahn, 2011). In contrast to the BHV (Billera *et al.*, 2001) or Robinson–Foulds metrics (Robinson & Foulds, 1981), the tropical interpretation of tree space provides both interpretable geometry and computational efficiency (Steel & Penny, 1993; Monod *et al.*, 2018). Many of the statistical methods defined for the tropical setting are framed as optimization problems (Barnhill *et al.*, 2024), and in this subsection we review some such tropical statistical optimization problems which we use to test our tropical descent methodology. We note the varying degrees of convexity demonstrated by each of them. While we restrict our considerations through the rest of this paper to statistics which arise from tropical location problems, in [Appendix A](#) we discuss other tropical statistical optimization problems.

2.3.1 Centrality Statistics

Our first problems of interest, Fermat–Weber points and Fréchet means, are centrality statistics for data on a general metric space; Fermat–Weber points (Drezner *et al.*, 2004) act as a generalized median, while Fréchet means (Fréchet, 1948) are a generalization of the mean.

Definition 19 (Tropical Fermat–Weber Points (Lin & Yoshida, 2018)). Let $X = \{\mathbf{x}_1, \dots, \mathbf{x}_K\} \subset \mathbb{R}^N / \mathbb{R}\mathbf{1}$ be our dataset. A solution to the following optimization problem is a *tropical Fermat–Weber point*:

$$\min_{\mathbf{t} \in \mathbb{R}^N / \mathbb{R}\mathbf{1}} f(\mathbf{t}) = \frac{1}{K} \sum_{k \leq K} d_{\text{tr}}(\mathbf{x}_k, \mathbf{t}).$$

Definition 20 (Tropical Fréchet means (Monod *et al.*, 2018)). Let $X = \{\mathbf{x}_1, \dots, \mathbf{x}_K\} \subset \mathbb{R}^N / \mathbb{R}\mathbf{1}$ be our dataset. A solution to the following optimization problem is a *tropical Fréchet mean*:

$$\min_{\mathbf{t} \in \mathbb{R}^N / \mathbb{R}\mathbf{1}} f(\mathbf{t}) = \left[\frac{1}{K} \sum_{k \leq K} d_{\text{tr}}(\mathbf{x}_k, \mathbf{t})^2 \right]^{1/2}.$$

The Fermat–Weber and Fréchet mean problems are both max-tropical and min-tropical location problems, as the tropical metric d_{tr} is both Δ_{\min} and Δ_{\max} -star-quasi-convex. In fact, they are also both classically convex and hence act as a benchmark against which we can test our gradient methods.

2.3.2 Wasserstein Projections

The next statistical optimization problem was motivated by Cai & Lim (2022), and looks to identify a tropical projection which minimizes the Wasserstein distance between samples in different tropical projective tori.

Definition 21 (Tropical Wasserstein Projections (Talbut *et al.*, 2023)). Let $X = \{\mathbf{x}_1, \dots, \mathbf{x}_K\} \subset \mathbb{R}^N/\mathbb{R}\mathbf{1}$ be a dataset in one space, and $Y = \{\mathbf{y}_1, \dots, \mathbf{y}_K\} \subset \mathbb{R}^M/\mathbb{R}\mathbf{1}$ be a dataset in a different space. Let J_1, \dots, J_M be a non-empty partition of $[N]$. Then the *tropical p -Wasserstein projection problem* is the minimization of the following objective function:

$$\min_{\mathbf{t} \in \mathbb{R}^N/\mathbb{R}\mathbf{1}} f_p(\mathbf{t}) = \left(\frac{1}{K} \sum_{k \leq K} \left\| (\max_{i \in J_j} (\mathbf{x}_k - \mathbf{t}))_{j \leq M} - \mathbf{y}_k \right\|_{\text{tr}}^p \right)^{1/p}$$

The *tropical ∞ -Wasserstein projection problem* is the minimization of:

$$\min_{\mathbf{t} \in \mathbb{R}^N/\mathbb{R}\mathbf{1}} f_\infty(\mathbf{t}) = \max_{k \leq K} \left\| (\max_{i \in J_j} (\mathbf{x}_k - \mathbf{t}))_{j \leq M} - \mathbf{y}_k \right\|_{\text{tr}}$$

In contrast to the work by Lee *et al.* (2022) which looks to solve the optimal transport problem for intrinsic measures on $\mathbb{R}^N/\mathbb{R}\mathbf{1}$, this p -Wasserstein projection problem is computing an optimal projection for empirical samples.

Proposition 22. *The tropical p, ∞ -Wasserstein projections are min-tropical location problems, and the ∞ -Wasserstein projection has min-tropically convex sub-level sets.*

Proof Let $\mathbf{z}_k = (x_{ki} - y_{kj})_{i \leq N}$ where j is such that J_j is the unique partition set containing i . We then have that

$$\begin{aligned} \left\| (\max_{i \in J_j} (\mathbf{x}_k - \mathbf{t}))_{j \leq M} - \mathbf{y}_k \right\|_{\text{tr}} &= \max_b \max_{a \in J_b} (z_{ka} - t_a) - \min_j \max_{i \in J_j} (z_{ki} - t_i) \\ &= \max_a (z_{ka} - t_a) + \max_j \min_{i \in J_j} (t_i - z_{ki}) \\ &= \max_j (\min_{i \in J_j} (t_i - z_{ki} - \min_a (t_a - z_{ka}))) \end{aligned}$$

The p, ∞ -Wasserstein projections can then be written as

$$\begin{aligned} f_p(\mathbf{t}) &= \left(\frac{1}{K} \sum_{k \leq K} \left(\max_j \min_{i \in J_j} (t_i - z_{ki} - \min_a (t_a - z_{ka})) \right)^p \right)^{1/p} \\ f_\infty(\mathbf{t}) &= \max_{k \leq K} \max_j \min_{i \in J_j} (t_i - z_{ki} - \min_a (t_a - z_{ka})) \end{aligned}$$

These are max-tropical location problems with:

$$\begin{aligned} g_p(\mathbf{h}) &= \left(\frac{1}{K} \sum_{k \leq K} h_k^p \right)^{1/p}, \\ g_\infty(\mathbf{h}) &= \max_{k \leq K} h_k, \\ h_k(\mathbf{t}) &= \hat{\gamma}(\mathbf{t} - \mathbf{z}_k), \\ \gamma(\mathbf{t}) &= \max_j \min_{i \in J_j} t_i. \end{aligned}$$

The g_p, g_∞ and γ are increasing in each coordinate and each h_k has kernel \mathbf{z}_k , satisfying the conditions for a min-tropical location problem.

As the h_k are Δ_{\min} -star-convex, their sub-level sets are min-tropically convex by Theorem 15. This is preserved when taking a maximum over samples, so f_∞ also has min-tropically convex sub-level sets. \square

Figure 4 shows a heatmap for the ∞ -Wasserstein projection objectives. As in the tropical linear regression problem, it is piecewise linear, non-convex and has sparse gradient.

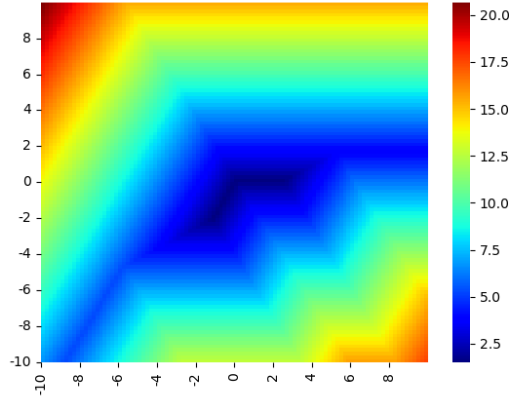


Figure 4: A heat map of a 3-sample ∞ -Wasserstein projection objective on $\mathbb{R}^3/\mathbb{R}\mathbf{1} \cong \mathcal{H} = \{\mathbf{x} : \sum x_i = 0\}$.

3 Steepest Descent with the Tropical Norm

This section comprises the theoretical contributions of this paper; we outline our proposed method of tropical descent, and the theoretical convergence guarantees for tropical descent when applied to tropical location problems.

We treat optimization over $\mathbb{R}^N/\mathbb{R}\mathbf{1}$ as optimization over \mathbb{R}^N with the knowledge that f is constant along $\mathbf{1}$ -rays. We assume we can compute some gradient-like function $\nabla f : \mathbb{R}^N \rightarrow \mathbb{R}^N$ which satisfies [Theorem 23](#).

Assumption 23. *Let $f = g(h_1, \dots, h_K)$ be a min-tropical location problem. Then we have that*

$$\nabla f(\mathbf{t})_j < 0 \Rightarrow \exists k \text{ s.t. } j \in \operatorname{argmin}_i (t_i - x_{ki}).$$

This is a very general assumption, which holds for some of the most natural gradient-like functions. For example, if $\nabla f(\mathbf{t})$ is given by some Clarke gradient, that is, some element of the *generalized Clarke derivative* of f , then [Theorem 25](#) shows that [Theorem 23](#) holds.

Definition 24 (Generalized Clarke Derivative (2.13, I.I of Kiwiel (1985))). We define the set $M_f(\mathbf{t})$ by

$$M_f(\mathbf{t}) = \{\mathbf{z} \in \mathbb{R}^N : \nabla f(\mathbf{y}_\ell) \rightarrow \mathbf{z}, \text{ where } \mathbf{y}_\ell \rightarrow \mathbf{t}, f \text{ differentiable at each } \mathbf{y}_\ell\}.$$

Then the *generalized Clarke derivative* is given by

$$\partial f(\mathbf{t}) = \operatorname{conv} M_f(\mathbf{t}).$$

Lemma 25. *Suppose $f = g(h_1, \dots, h_K)$ is min-tropical location problem, and for all \mathbf{t} , $\nabla f(\mathbf{t})$ is some element of $\partial f(\mathbf{t})$. Then [Theorem 23](#) holds.*

Proof Suppose that $\nabla f(\mathbf{t})_j < 0$. Then there is a sequence of differentiable \mathbf{y}_ℓ satisfying $\nabla f(\mathbf{y}_\ell)_j < 0$, $\mathbf{y}_\ell \rightarrow \mathbf{t}$. Hence by the chain rule, as g is increasing in every h_k , there is some h_k which is strictly decreasing in the j^{th} coordinate at \mathbf{y}_ℓ . WLOG, the same h_k is strictly decreasing in the j^{th} coordinate for all \mathbf{y}_ℓ . As γ is increasing in every coordinate, $h_k = \hat{\gamma}(\mathbf{y}_\ell - \mathbf{x}_k)$ is strictly decreasing in the j^{th} coordinate if and only if $j \in \operatorname{argmin}_i (y_{\ell i} - x_{ki})$. This is preserved through the limit as $\ell \rightarrow \infty$, so we conclude that $j \in \operatorname{argmin}_i (t_i - x_i)$. \square

In practice, rather than computing elements of the generalized Clarke derivative, we use PyTorch automatic differentiation (Paszke *et al.*, 2019). The derivatives computed by PyTorch are dependent on the computational representation of a function, but are designed to respect the chain rule. We must therefore ensure that our computational representation of g has non-negative derivatives in each h_k , while each h_k is

computed such that its t_j derivative is negative only if $j \in \operatorname{argmin}_i(t_i - x_{ki})$. For such a computational representation of f , [Theorem 23](#) will hold by the chain rule. For all the tropical location problems we consider in this paper, we find their most natural computational representation gives rise to derivatives ∇f satisfying [Theorem 23](#).

3.1 Proposed Method

In defining tropical descent, we refer back to the motivation behind classical gradient descent—steepest descent directions.

Definition 26 (Steepest Descent Direction (Boyd & Vandenberghe, 2004)). A normalized *steepest descent direction* at \mathbf{t} with respect to the norm $\|\cdot\|$ is:

$$\mathbf{d} = \operatorname{argmin}\{\nabla f(\mathbf{t})^\top \mathbf{v} : \|\mathbf{v}\| = 1\}.$$

With respect to the Euclidean norm, the normalized derivative is a steepest descent direction. The steepest descent directions under the tropical norm are characterized by the following lemma.

Lemma 27. *Suppose $\nabla f \neq \mathbf{0}$. Then the direction \mathbf{v} is a normalized tropical steepest descent direction (up to \sim equivalence) iff*

$$\begin{aligned} \nabla f_i < 0 &\Rightarrow v_i = 1, \\ \nabla f_i > 0 &\Rightarrow v_i = 0. \end{aligned}$$

Proof WLOG, we assume $0 \leq v_i \leq 1$. Then

$$\nabla f^\top \mathbf{v} \geq \sum_{i: \nabla f_i < 0} \nabla f_i$$

This is achieved if and only if $v_i = 1$ for all i such that $\nabla f_i < 0$, and $v_i = 0$ for all i such that $\nabla f_i > 0$. We note that any such v_i satisfies $\|\mathbf{v}\|_{\text{tr}} = 1$ as $\sum_i \nabla f_i = 0$ by the equivalence relation of the tropical projective torus, and $\nabla f_i \neq 0$ so ∇f has positive and negative coordinates. \square

[Theorem 27](#) uniquely defines a descent direction \mathbf{d} if and only if, for every coordinate i , $\nabla f_i \neq 0$. To uniquely define a descent direction for any \mathbf{t} , we take the direction \mathbf{d} given by

$$d_i = \begin{cases} 1 & \text{if } \nabla f_i < 0, \\ 0 & \text{otherwise.} \end{cases}$$

We refer to this as a *min-tropical descent* direction. In contrast,

$$d_i = \begin{cases} -1 & \text{if } \nabla f_i > 0, \\ 0 & \text{otherwise.} \end{cases}$$

defines a *max-tropical descent* direction.

Throughout the rest of this paper, we use the min-tropical descent direction as convention, and will specify when the max-tropical descent direction is used instead. Tropical descent therefore refers to the method outlined by [Algorithm 1](#), for some specified step size sequence $(a_m)_{m \geq 1}$, while we refer to classical gradient descent as classical descent.

We note that over a large number of steps, [Algorithm 1](#) can produce large t_{mi} values as each coordinate is non-decreasing in m . If this results in overflow or precision errors, a normalization operation can be included in each step, such as subtracting $\frac{1}{N} \sum_{i \leq N} t_{mi}$ from each t_{mi} . The function f is invariant under such a translation due to the equivalence relation on the tropical projective torus.

We note that Sabol *et al.* (2024) and Barnhill *et al.* (2024) implement classical descent for the computation of Fermat–Weber points; this is the most natural choice as the Fermat–Weber problem is classically convex. However, the linear regression and Wasserstein projection problems lack classical convexity, and hence do not consistently produce accurate solutions via classical descent. It is these tropically convex problems for which tropical descent is necessary.

Algorithm 1 Tropical Descent

for $m < \text{max_steps}$ **do**
 $\mathbf{g}_{mi} \leftarrow \nabla f(\mathbf{t}_{m-1})_i;$
 $\mathbf{d}_{mi} \leftarrow \mathbf{1}_{\mathbf{g}_{mi} < 0};$
 $\mathbf{t}_m \leftarrow \mathbf{t}_{m-1} + a_m \mathbf{d}_m;$

3.2 Convergence Guarantees

In this section we prove the theoretical guarantees of tropical descent for min-tropical location problems. We show that tropical descent must converge to the tropical convex hull of the data, and hence will necessarily find a minimum of a Δ_{\min} -star-convex problem. Throughout this section, we assume the step sizes a_m satisfy $a_m \rightarrow 0, \sum a_m = \infty$.

We first highlight the key difference in stability between classical descent and tropical descent; if some component of the derivative is locally zero, tropical descent cannot converge in that neighborhood.

Proposition 28. *Let \mathbf{t}_m be some sequence defined by tropical descent. Assume that for all $m, \nabla f(\mathbf{t}_m) \neq \mathbf{0}$. Suppose in some bounded open $U, \nabla f_i$ is identically 0. Then no point in U is a convergence point for \mathbf{t}_m ; in particular, if $\mathbf{t}_m \in U$ there is some $n > m$ such that $\mathbf{t}_n \notin U$.*

Proof Assume otherwise. Then for all $n \geq m$, we have $\nabla f(\mathbf{t}_n)_i = 0$, so t_{ni} is constant. At each step, we increase at least one coordinate by a_n , so as $n \rightarrow \infty$:

$$\sum_j t_{nj} \geq \sum_j t_{mj} + \sum_{n \geq m'} a_{m'} \rightarrow \infty.$$

Therefore $\|\mathbf{t}_n\|_{\text{tr}}$ will become arbitrarily large, as $\max_j t_{nj} \rightarrow \infty$ while $\min_j t_{nj} \leq t_{mi}$. Then we must have left U ; contradiction. \square

As a result of the proposition above, local minima such as the valleys in [Figures 3 and 4](#) can be stable with respect to classical descent but unstable with respect to tropical descent.

We next prove the main convergence result of this work; tropical descent must converge to the tropical convex hull of the data points.

Theorem 29. *Suppose f is a min-tropical location problem with respect to the dataset $X = \{\mathbf{x}_1, \dots, \mathbf{x}_K\}$. Let $(\mathbf{t}_m)_{m \geq 1}$ be a sequence of points defined by tropical descent, such that for all $m: \nabla f(\mathbf{t}_m) \neq \mathbf{0}$. Let $V = \text{tconv}_{\max}(\mathbf{x}_1, \dots, \mathbf{x}_K)$, and define*

$$\Delta_j(\mathbf{t}) = \sum_{k \leq K} \sum_{i \leq N} [t_j - x_{kj} - t_i + x_{ki}]^+.$$

For any $\epsilon > 0$, let M_1 be such that for all $m \geq M_1, a_m < \epsilon/N$. Let M_2 be such that for all $m \geq M_2, s_m \geq \max_j \Delta_j(\mathbf{t}_{M_1}) + s_{M_1} - K\epsilon$, where s_m is the partial sum of the step size sequence a_m . Then for all $m \geq M_2$ we have:

$$d_{\text{tr}}(\mathbf{t}_m, V) \leq \epsilon.$$

Proof For each $i \leq N$, we define the functions

$$\delta_j(\mathbf{t}) = \min_{k \leq K} \left[\sum_{i \leq N} [t_j - x_{kj} - t_i + x_{ki}]^+ \right].$$

Claim 30. *For all $\mathbf{t} \in \mathbb{R}^N / \mathbb{R}\mathbf{1}$, we have $d_{\text{tr}}(\mathbf{t}, V) \leq \max_j \delta_j(\mathbf{t})$.*

Proof As discussed by Maclagan & Sturmfels (2015), there is a well-defined metric projection map π_V onto V given by:

$$\pi_V(\mathbf{t}) = \lambda_1 \odot \mathbf{x}_1 \boxplus \dots \boxplus \lambda_K \odot \mathbf{x}_K,$$

where $\lambda_k = \max\{\lambda \in \mathbb{R} : \lambda \odot \mathbf{x}_k \boxplus \mathbf{t} = \mathbf{t}\} = \min_i (t_i - x_{ki})$.

The distance from \mathbf{t} to V is then given by $d(\mathbf{t}, \pi_V(\mathbf{t}))$, and we have:

$$\begin{aligned} d(\mathbf{t}, V) &= d(\mathbf{t}, \pi_V(\mathbf{t})) \\ &= \left\| \left(\max_k \left(\min_i (t_i - x_{ki}) - t_j + x_{kj} \right) \right)_{j \leq N} \right\|_{\text{tr}}. \end{aligned}$$

We note that for all j, k , the term $\min_i (t_i - x_{ki}) - t_j + x_{kj}$ is negative. Hence:

$$\begin{aligned} d(\mathbf{t}, V) &\leq 0 - \min_j \left(\max_k \left(\min_i (t_i - x_{ki}) - t_j + x_{kj} \right) \right) \\ &= \max_j \left(\min_k \left(t_j - x_{kj} - \min_i (t_i - x_{ki}) \right) \right) \\ &\leq \max_j \delta_j(\mathbf{t}). \end{aligned}$$

The claim is proved. \square

We will now prove that for all $m \geq M_2$, we have that $\delta_j(\mathbf{t}_m) \leq \epsilon$.

Claim 31. *If $\delta_i(\mathbf{t}_m) = 0$ and $m \geq M_1$, then $\delta_i(\mathbf{t}_{m+1}) < \epsilon$.*

Proof For all $k \leq K, j \leq N$, we have that $t_{mj} - x_{kj} - t_{mi} + x_{ki}$ is 1-Lipschitz in \mathbf{t} (with respect to d_{tr}). Therefore δ_j is N -Lipschitz in \mathbf{t} . By the tropical descent rule:

$$\begin{aligned} \delta_j(\mathbf{t}_{m+1}) &\leq \delta_j(\mathbf{t}_m) + N d_{\text{tr}}(\mathbf{t}_m, \mathbf{t}_{m+1}) \\ &= 0 + N a_m \\ &< \epsilon. \end{aligned}$$

The claim is proved. \square

Claim 32. *If $\delta_j(\mathbf{t}_m) > 0$ then $\delta_j(\mathbf{t}_{m+1}) \leq \delta_j(\mathbf{t}_m)$.*

Proof Suppose $\delta_j(\mathbf{t}_m) > 0$. Then $\forall k, t_{mj} - x_{kj} > \min_i (t_{mi} - x_{ki})$, so by [Theorem 25](#) we have $\nabla f_j \geq 0$. The tropical steepest descent direction therefore has $d_{mj} = 0$. We conclude that

$$\begin{aligned} \forall k, i: \quad t_{(m+1)j} - x_{kj} - t_{(m+1)i} + x_{ki} &\leq t_{mj} - x_{kj} - t_{mi} + x_{ki}, \\ \Rightarrow \delta_j(\mathbf{t}_{m+1}) &\leq \delta_j(\mathbf{t}_m). \end{aligned}$$

The claim is proved. \square

Claim 33. *For some $M_1 \leq m \leq M_2$, $\delta_j(\mathbf{t}_m) < \epsilon$.*

Proof We note that $K\delta_j(\mathbf{t}) \leq \Delta_j(\mathbf{t})$; hence if $\Delta_j(\mathbf{t}_{M_1}) < K\epsilon$ then we are done.

We assume $\delta_j(\mathbf{t}_m) > \epsilon$ for all $M_1 \leq m \leq M_2$, and prove the result by contradiction. Then as in the proof of the previous claim, at each step we have $\nabla f_j \geq 0$, $d_{mj} = 0$ and t_{mj} is fixed for $M_1 \leq m \leq M_2$.

We have assumed that for each m , $\nabla f \neq \mathbf{0}$ and so there is some i such that $\nabla f_i < 0$, and by [Theorem 25](#), there is some k such that $i \in \text{argmin}_\ell (t_{m\ell} - x_{k\ell})$. Hence:

$$\begin{aligned} \forall \ell: \quad t_{mj} - x_{kj} - t_{mi} + x_{ki} &\geq t_{mj} - x_{kj} - t_{m\ell} + x_{k\ell}, \\ \Rightarrow \quad t_{mj} - x_{kj} - t_{mi} + x_{ki} &\geq \delta_j(\mathbf{t}_m)/N, \\ &> \epsilon/N, \\ &\geq a_m. \end{aligned}$$

Hence this term in the summation of $\Delta_j(\mathbf{t}_m)$ decreases by a_m , while other terms are non-increasing as t_{mj} is fixed.

Noting that $K\delta_j(\mathbf{t}) \leq \Delta_j(\mathbf{t})$, we conclude

$$\begin{aligned} K\delta_j(\mathbf{t}_{M_2}) &\leq \Delta_j(\mathbf{t}_{M_2}), \\ &\leq \Delta_j(\mathbf{t}_{M_1}) - s_{M_2} + s_{M_1}, \\ &\leq K\epsilon. \end{aligned}$$

Contradiction. So the claim is proved. \square

Finally, from the claims above, we conclude that $\forall m \geq M_2, i \leq N$, we have $\delta_i(\mathbf{t}_m) \leq \epsilon$, and so by our first claim, we have $d_{\text{tr}}(\mathbf{t}_m, V) \leq \epsilon$. \square

As proven by Comănesci (2024), tropical location problems have minima in the tropical convex hull of the data. The theorem above says that according to tropical descent, only such minima can be stable. We cannot do much better in terms of convergence results for general location problems; they can have disconnected sub-level sets so we would not expect gradient methods to find a global minimum. We would require some degree of convexity to guarantee global solvability, which is exactly what the following corollary gives us; tropical descent will necessarily converge to a minimum of any Δ_{\min} -star-quasi-convex function.

Corollary 34. *Let $f(\mathbf{t})$ be a Δ_{\min} -star-quasi-convex function, and let $(\mathbf{t}_m)_{m \geq 1}$ be a sequence of points defined by tropical descent such that for all m : $\nabla f(\mathbf{t}_m) \neq \mathbf{0}$. Then there is some global minimum \mathbf{t}^* such that for all $m \geq M_2$, $d_{\text{tr}}(\mathbf{t}_m, \mathbf{t}^*) \leq \epsilon$ where M_2 is as in Theorem 29.*

This corollary follows from considering the 1-sample case of tropical location problems; Theorem 34 establishes convergence to the kernel of a Δ_{\min} -star-quasi-convex function, which must necessarily be a global minimum. This convergence result holds even if f does not have a unique minimum — it may be that f has multiple global minima but a unique kernel, or f may have a full dimensional set of global minima upon which $\nabla f(\mathbf{t}) = \mathbf{0}$ and tropical descent terminates.

As a further corollary, we note that we can achieve the same result for max-tropical location problems by using max-tropical descent directions.

Corollary 35. *Suppose f is a max-tropical location problem with respect to the dataset $X = \{\mathbf{x}_1, \dots, \mathbf{x}_K\}$. Let $(\mathbf{t}_m)_{m \geq 1}$ be a sequence of points defined via max-tropical descent directions, such that for all m : $\nabla f(\mathbf{t}_m) \neq \mathbf{0}$. Let $V = \text{tconv}_{\min}(\mathbf{x}_1, \dots, \mathbf{x}_K)$, and define*

$$\Delta'_i(\mathbf{t}) = \sum_{k \leq K} \sum_{j \leq N} [t_j - x_{kj} - t_i + x_{ki}]^+.$$

For any initial \mathbf{t}_0 and $\epsilon > 0$, let M_1 be such that for all $m \geq M_1$, $a_m \leq \epsilon/N$. Let M_2 be such that for all $m \geq M_2$ $s_m \geq \max_i \Delta'_j(\mathbf{t}_{M_1}) + s_{M_1} - K\epsilon$. Then for all $m \geq M_2$ we have:

$$d_{\text{tr}}(\mathbf{t}_m, V) \leq \epsilon.$$

Remark 36. The results above indicate convergence to V or \mathbf{t}^* in the tropical topology of $\mathbb{R}^N/\mathbb{R}\mathbf{1}$, but \mathbf{t}_m cannot converge in the Euclidean topology of \mathbb{R}^N due to the divergent partial sums of a_m .

We conclude by establishing a foundational bound for the convergence rate of tropical descent; we take step sizes given by $a_m = \alpha m^{-1/2} \|\nabla f(\mathbf{t}_m)\|_{\text{tr}}$, and assume derivatives have bounded tropical norm as is the case for piecewise linear 1-Lipschitz objective functions (with finitely many linear pieces). In this case, we prove convergence at a rate of $O(1/\sqrt{m})$.

Proposition 37. *Suppose f is a min-tropical location problem as in Theorem 29. Assume that there is some $L \in \mathbb{N}$ such that for all \mathbf{t}_m , $1/L \leq \|\nabla f(\mathbf{t}_m)\|_{\text{tr}} \leq 2$, and assume further there is some D such that $\forall m \in \mathbb{N}$: $\sum_{k \leq K} d_{\Delta_{\max}}(\mathbf{x}_k, \mathbf{t}_m) \leq KD$. We define $a_m = \alpha m^{-1/2} \|\nabla f(\mathbf{t}_m)\|_{\text{tr}}$. Then for all m satisfying*

$$m \geq \max \left\{ \left(\sqrt{2} + \frac{KDL}{2\alpha} - \sqrt{LKN - 1} \right)^2 - 1, \left(\frac{2\alpha N}{D} \right)^2 \right\}, \quad (2)$$

we have that:

$$d_{\text{tr}}(\mathbf{t}_m, V) \leq \frac{2\sqrt{2}\alpha N}{\sqrt{m+1} - KDL/2\alpha + \sqrt{LKN - 1} - \sqrt{2}} = \epsilon_m.$$

In particular, if f is a Δ_{\min} -star-quasi-convex function, then there is some global minimum \mathbf{t}^* such that

$$d_{\text{tr}}(\mathbf{t}_m, \mathbf{t}^*) \leq \frac{2\sqrt{2}\alpha N}{\sqrt{m+1} - DL/2\alpha + \sqrt{LN - 1} - \sqrt{2}} = \epsilon'_m.$$

In order to use [Theorem 29](#), we will need to find some M_1 such that $a_{M_1} < \epsilon/N$ (our step size is small enough) and $s_m \geq \max_j \Delta_j(\mathbf{t}_{M_1}) + s_{M_1} - K\epsilon$ (we have taken enough steps to get close to V). Our condition that m is large enough such that $\sqrt{m+1} - KDL/2\alpha + \sqrt{LKN-1} \geq \sqrt{2}$ ensures that such an M_1 exists, while $\sqrt{m} \geq 2\alpha N/D$ ensures that $M_1 \leq m$. We can then take the largest such M_1 to ensure that the corresponding ϵ is as tight as possible.

Proof We fix m satisfying [\(2\)](#) and define:

$$\xi(m) := \frac{\sqrt{m+1}}{2} - \frac{KDL}{4\alpha} + \sqrt{\left(\frac{\sqrt{m+1}}{2} - \frac{KDL}{4\alpha}\right)^2 + LKN - 1},$$

$$M_1 := \lfloor \xi(m)^2 \rfloor.$$

We first note that by the quadratic mean inequality and as $\sqrt{m+1} - KDL/2\alpha + \sqrt{LKN-1} \geq \sqrt{2}$:

$$\begin{aligned} \xi(m) &= \frac{\sqrt{m+1}}{2} - \frac{KDL}{4\alpha} + \sqrt{\left(\frac{\sqrt{m+1}}{2} - \frac{KDL}{4\alpha}\right)^2 + LKN - 1} \\ &\geq \frac{\sqrt{m+1}}{2} - \frac{KDL}{4\alpha} + \frac{1}{\sqrt{2}} \left(\frac{\sqrt{m+1}}{2} - \frac{KDL}{4\alpha} + \sqrt{LKN-1} \right) \\ &\geq \frac{1}{\sqrt{2}} \left(\sqrt{m+1} - \frac{KDL}{2\alpha} + \sqrt{LKN-1} \right) \geq 1. \end{aligned}$$

Therefore we have that

$$1 \leq \sqrt{M_1} \leq \xi(m),$$

and so $\sqrt{M_1}$ lies between the roots of the polynomial

$$p(t) = L^{-1}t^2 + (KD/2\alpha - L^{-1}\sqrt{m+1})t + L^{-1} - KN.$$

Therefore:

$$\begin{aligned} L^{-1}(M_1 + 1) + (KD/2\alpha - L^{-1}\sqrt{m+1})\sqrt{M_1} - KN &\leq 0, \\ L^{-1}\sqrt{M_1}\sqrt{M_1+1} + KD\sqrt{M_1}/2\alpha - L^{-1}\sqrt{M_1}\sqrt{m+1} &\leq KN, \\ KD + 2\alpha L^{-1}(\sqrt{M_1+1} - \sqrt{m+1}) &\leq \frac{2\alpha KN}{\sqrt{M_1}}. \end{aligned}$$

We now show that $M_1 \leq m$. Suppose otherwise; then by the inequality above:

$$\begin{aligned} KD &\leq \frac{2\alpha KN}{\sqrt{M_1}} + 2\alpha L^{-1}(\sqrt{m+1} - \sqrt{M_1+1}) \\ &< \frac{2\alpha KN}{\sqrt{m}} \end{aligned}$$

This contradicts our assumption that $m \geq (2\alpha N/D)^2$, so we conclude that $M_1 \leq m$.

Claim 38. For all $n \geq m$ we have $a_n \leq \epsilon_m/N$.

Proof We have shown that $\xi(m) \geq 1$, so:

$$\begin{aligned} M_1 &\geq \xi(m)^2 - 1, \\ &\geq (\xi(m) - 1)^2, \\ \sqrt{M_1} &\geq \xi(m) - 1, \\ &\geq \frac{1}{\sqrt{2}} \left(\sqrt{m+1} - \frac{KDL}{2\alpha} + \sqrt{LKN-1} \right) - 1. \end{aligned}$$

Hence, by the step size definition and the fact that $n \geq m \geq M_1$:

$$\begin{aligned} a_n &\leq \frac{2\alpha}{\sqrt{M_1}}, \\ &\leq \frac{2\sqrt{2}\alpha}{\sqrt{m+1} - KDL/2\alpha + \sqrt{LKN-1} - \sqrt{2}} = \epsilon_m/N. \end{aligned}$$

The claim is proved. \square

Claim 39. We have $\max_j \Delta_j(\mathbf{t}_{M_1}) + s_{M_1} - s_m \leq K\epsilon_m$.

Proof We note that

$$\begin{aligned} \Delta_j(\mathbf{t}_{M_1}) &= \sum_{k \leq K} \sum_{i \leq N} [t_{M_1 j} - x_{kj} - t_{M_1 i} + x_{ki}]^+, \\ &\leq \sum_{k \leq K} d_{\Delta_{\max}}(\mathbf{x}_k, \mathbf{t}_{M_1}), \\ &\leq KD. \end{aligned}$$

And therefore we have $\max_j \Delta_j(\mathbf{t}_{M_1}) \leq KD$. The partial sums are bounded by:

$$\begin{aligned} s_{M_1} - s_m &\leq \sum_{n=M_1+1}^m -a_n \\ &\leq \sum_{n=M_1+1}^m \frac{-\alpha}{Ln^{1/2}} \\ &\leq \sum_{n=M_1+1}^m -2\alpha L^{-1}(\sqrt{n+1} - \sqrt{n}) \\ &\leq 2\alpha L^{-1}(\sqrt{M_1+1} - \sqrt{m+1}). \end{aligned}$$

Therefore:

$$\begin{aligned} \max_i \Delta_i(\mathbf{t}_{M_1}) + s_{M_1} - s_m &\leq KD + 2\alpha L^{-1}(\sqrt{M_1+1} - \sqrt{m+1}), \\ &\leq \frac{2\alpha KN}{\sqrt{M_1}} \leq K\epsilon_m. \end{aligned}$$

\square

Hence by [Theorem 29](#), we have that

$$d_{\text{tr}}(\mathbf{t}_m, V) \leq \epsilon_m.$$

The bound for the tropically quasi-convex case follows from [Theorem 34](#). \square

Our error bound in Proposition 12 is a useful foundational result on the convergence behavior of tropical descent; for sufficiently nice problems, tropical descent will converge at a rate of $O(1/\sqrt{m})$. However, a more detailed study of the numerical analysis of tropical descent would be valuable. We outline possible questions below, as well as presenting a comparison of our error bounds with tropical descent for tropical linear regression.

Firstly, the constant term $LD/2\alpha$ in the denominator of ϵ_m will typically be larger than necessary, resulting in a weaker error bound. In particular, this constant term is quick to dominate for larger problems. Further work improving these constant factors would produce much tighter and more robust error bounds. Secondly, the error ϵ_m bounds the distance to a tropical convex hull V , which is rarely a useful quantity to bound. We would rather use ϵ'_m , which bounds the distance to a global minimum, but our tropical location problems are not known to be Δ_{\min} -star-quasi-convex. It would be particularly useful to generalize our error bound ϵ'_m to such problems which exhibit some local (but not global) Δ_{\min} -star-quasi-convexity.

For a qualitative view on [Theorem 37](#), we compare ϵ'_m and the convergence rate of tropical descent for tropical linear regression. As noted, tropical linear regression is tropically quasi-convex ([Theorem 18](#)) but not known to be Δ_{\min} -star-quasi-convex, so does not meet the assumptions of [Theorem 37](#); despite this, we see ϵ'_m is often an effective upper bound on the error in \mathbf{t} .

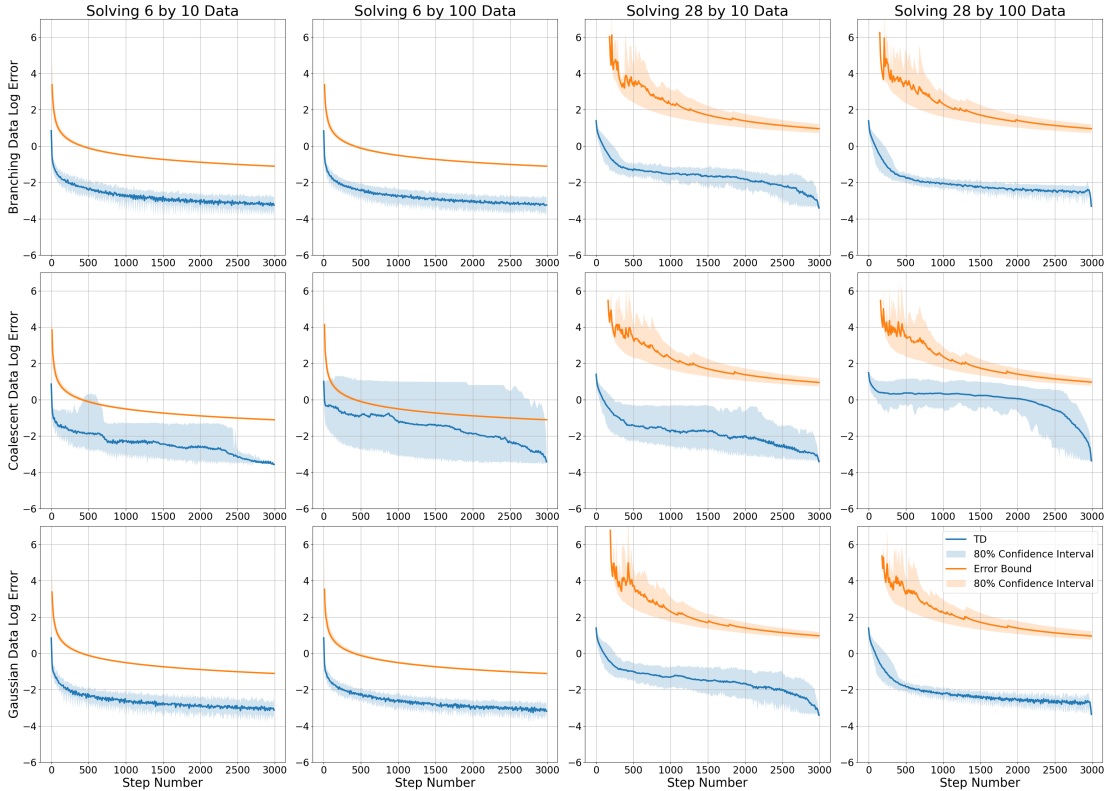


Figure 5: The mean log error bound $\log \epsilon'_m$ and the mean log tropical distance to the estimated minimum \mathbf{t}^* when applying tropical descent (TD) with $\alpha = 1$ to solve the tropical linear regression problem. For each dataset, we take 50 random initialization points and compute $\log \epsilon'_m$ and $\log d_{\text{tr}}(\mathbf{t}_m, \mathbf{t}^*)$ independently, then take an average. We also record the 10th and 90th percentile values to estimate an 80% confidence interval.

We perform tropical descent for tropical linear regression using 12 different datasets; these are generated via branching processes, coalescent processes, or a Gaussian distribution on $\mathbb{R}^6/\mathbb{R}\mathbf{1}$ and $\mathbb{R}^{28}/\mathbb{R}\mathbf{1}$. We consider sample sizes of 10 or 100. These are the same datasets used in [Section 4](#), and further details on their generation can be found in [Appendix B](#). We run computations using a learning rate of $\alpha = 1$, for steps up to $m \leq 3000$. The tropical linear regression problem has $\|\nabla f(\mathbf{t}_m)\| = 2$ almost everywhere, so we take $L = 1$ when computing ϵ'_m . We estimate \mathbf{t}^* to be the mean of the final 10 steps of tropical descent (TD), and compute a tight estimate for D by taking

$$D \approx \max_{m \leq 3000} d_{\Delta_{\max}}(\mathbf{t}^*, \mathbf{t}_m).$$

[Figure 5](#) shows the mean log error bound ϵ'_m with the mean log tropical distance to \mathbf{t}^* .

Examining [Figure 5](#), we first note that the error ϵ'_m is orders of magnitude smaller for the lower dimensional problems, which is primarily a result of the constant terms in the denominator of ϵ'_m . As we have noted, it would be of significant value to reduce these constant terms in future numerical analytical studies of tropical descent. These constant terms are also the cause of noise in the mean error bound for high dimensional problems, as we require more steps for the error to be well-defined. We also note that although ϵ'_m is a reasonable upper bound for the distance to \mathbf{t}^* in many cases, this upper bound does not hold for the

low dimensional coalescent datasets. It is unclear whether this is due to poor estimates for D and \mathbf{t}^* , or due to tropical linear regression not being Δ_{\min} -star-quasi-convex. We conclude by noting that we are observing a convergence rate of $O(1/\sqrt{m})$ for most experiments, with this rate appearing particularly distinctly for branching process and Gaussian data.

4 Numerical Experiments

In this section we compare the practical performance of classical descent, tropical descent, SGD, tropical SGD, Adam, Adamax, and tropical Adamax, with a focus on their stability behavior. The implementation for all these experiments is available in the GitHub repository at <https://github.com/Roroast/TropicalGradDescent>.

4.1 Methods

We begin by outlining our implementation of steepest descent, stochastic gradient descent (SGD), and Adam as well as their tropical variants. We take a heuristic approach to the tropicalization of SGD and Adam, replacing derivatives with tropical steepest descent directions in each case.

Steepest Descent. We will perform classical descent (CD) and tropical descent (TD) using equivalent step size sequences a_m for both methods, which we fix as

$$a_m = \frac{\gamma \|\nabla f(\mathbf{t}_m)\|}{\sqrt{m}},$$

where $\|\cdot\|$ is the Euclidean norm for classical descent and the tropical norm for tropical descent. When $\nabla f(\mathbf{t})$ is bounded this is a well-behaved step rule; a_m will converge to 0. Furthermore, for the piecewise linear problems, $\|\nabla f(\mathbf{t}_m)\|$ is bounded away from 0 almost everywhere which is not a global minimum, so $\sum a_m = \infty$.

Stochastic Gradient Descent. Stochastic gradient descent is a variant of gradient descent which looks to improve computational speed by approximating $\nabla f(\mathbf{t})$; rather than computing the loss and its derivative at \mathbf{t} with respect to the entire dataset $f(\mathbf{t}; X)$, we evaluate the loss and its derivative with respect to a random sample $\mathbf{x}_m \in X$, $f(\mathbf{t}; \mathbf{x}_m)$. This is simplified with the notation $f_m(\mathbf{t})$. As with gradient descent, we use the step size sequence given by

$$a_m = \frac{\gamma \|\nabla f_m(\mathbf{t}_m)\|}{\sqrt{m}},$$

where $\|\cdot\|$ is the Euclidean norm for stochastic gradient descent (SGD) and the tropical norm for tropical stochastic gradient descent (TSGD).

Adam Variants. The Adam algorithm (Kingma & Ba, 2015) uses gradient momentum to compound consistent but small effects. This is done by taking first and second moments of the gradient over all steps using exponentially decaying weights. The Adamax algorithm is a variant of the Adam algorithm motivated by the use of the ∞ -moments rather than second moments.

To adapt the Adam algorithm for the tropical setting, we take moments of an unnormalized tropical descent direction. When looking to take higher moments of the gradient over m , the L_∞ is the natural option for the tropical setting. We therefore look to use the Adamax recursion relation on the ∞ -moment estimate \mathbf{u}_m :

$$\mathbf{u}_{m+1} = \max(\beta_2 \mathbf{u}_m, \mathbf{d}_m).$$

The tropicalized Adamax algorithm is then given by [Algorithm 2](#).

4.2 Computation

We now look to solve our centrality statistics, Wasserstein projection problems, and tropical linear regression using the 7 gradient methods discussed: classical descent (CD), tropical descent (TD), stochastic gradient descent (SGD), tropical stochastic gradient descent (TSGD), Adam, Adamax, and TrAdamax. We run computations for 12 datasets of different sizes, shapes and dimensions; motivated by phylogenetic data

Algorithm 2 TrAdamax

```
v, u  $\leftarrow$  0;  
for  $m < \text{max\_steps}$  do  
   $\mathbf{g}_{mi} \leftarrow \nabla f(\mathbf{t}_{m-1})_i$ ;  
   $\mathbf{d}_{mi} \leftarrow (\max_j(\mathbf{g}_{mj}) - \min_j(\mathbf{g}_{mj})) * \mathbf{1}_{\mathbf{g}_{mi} > 0}$ ;  
   $\mathbf{v}_m \leftarrow \beta_1 * \mathbf{v}_{m-1} + (1 - \beta_1) * \mathbf{d}_m$ ;  
   $\mathbf{u}_m \leftarrow \max(\beta_2 * \mathbf{u}_{m-1}, |\mathbf{d}_m|)$ ;  
   $\mathbf{t}_m \leftarrow \mathbf{t}_m - \alpha / (1 - \beta_1^m) * \mathbf{v}_m / \mathbf{u}_m$ ;
```

science applications, we consider datasets generated by branching processes, coalescent processes, or Gaussian distributions on $\mathbb{R}^N/\mathbb{R}\mathbf{1}$, for $N = 6, 28$ and samples of size 10 or 100. We take the same random initializations for each gradient method, taken from a Gaussian distribution on \mathbb{R}^N . [Appendix B](#) provides further details on the simulated datasets and computational methodology used. For each gradient method, we use learning rates which have been optimized for each dataset size and dimension, across different distribution types ([Appendix C](#)).

Rather than investigating the relative convergence rates of each method, we are interested in the relative stability of local minima. We therefore plot the CDF of the relative log error after 1000 steps over 50 random initializations, to reveal concentrations of error values where multiple initializations stabilize. When the CDF of one method dominates another, it has a higher probability of achieving the same error or less and is therefore a more suitable method.

As we will observe, tropical gradient methods are stable at fewer points than classical gradient methods; as a result, tropical methods typically have further to travel before reaching a stable point. Over few steps, this would be compensated for by selecting larger learning rates for tropical gradient methods relative to classical gradient methods, leading to less precise results in the case of tropical gradient methods. Our computations are run over 1000 steps, as this gives enough time for tropical gradient methods to stabilize, given our initializations, without sacrificing learning rate; we see in [Appendix C](#) that neither classical nor tropical learning rates are consistently greater than the other.

4.2.1 Centrality Statistics

We first consider the behavior of tropical descent methods for Fermat–Weber points and Fréchet means. These optimization problems are classically convex problems, as well as being both max-tropical and min-tropical location problems, and therefore lend themselves well to gradient methods. The experimental behavior of these problems is similar, so in this section we include the results for the Fermat–Weber problem while the results for Fréchet means can be found in [Appendix E](#).

[Figure 6](#) shows the CDF of the log relative error after 1000 steps of each gradient method for the 12 datasets. We note that the deterministic methods achieve similar results for most datasets, while the stochastic methods achieve the worst error for all 12 datasets and TSGD is performing worse than SGD. The disparity between SGD and TSGD is greatest when the dimensionality of the data is greater than the size of the dataset, and for coalescent data. We see similar behavior in the log error of tropical descent and TrAdamax; they perform on par with their classical counterparts for each dataset other than the 28 by 10 coalescent data, for which the tropical gradient methods are not achieving the same accuracy ([Table 1](#)). While it is unclear why this is, we note that coalescent data is supported on the space of ultrametric trees, which is a tropical hyperplane (Ardila & Klivans, 2006; Page *et al.*, 2020) and may influence the stability of minima.

4.2.2 Wasserstein Projections

The Wasserstein projection problems highlight the differences in stability behavior between classical and tropical gradient methods, as they are min-tropical location problems but not classically convex. The CDFs of the final log relative errors can be found in [Figures 7](#) and [8](#).

In [Figures 7](#) and [8](#) we see large steps at various intervals in the CDF plots, which is indicative of stable local minima. This is particularly prevalent in low dimensional space. Classical descent, Adam, and Adamax

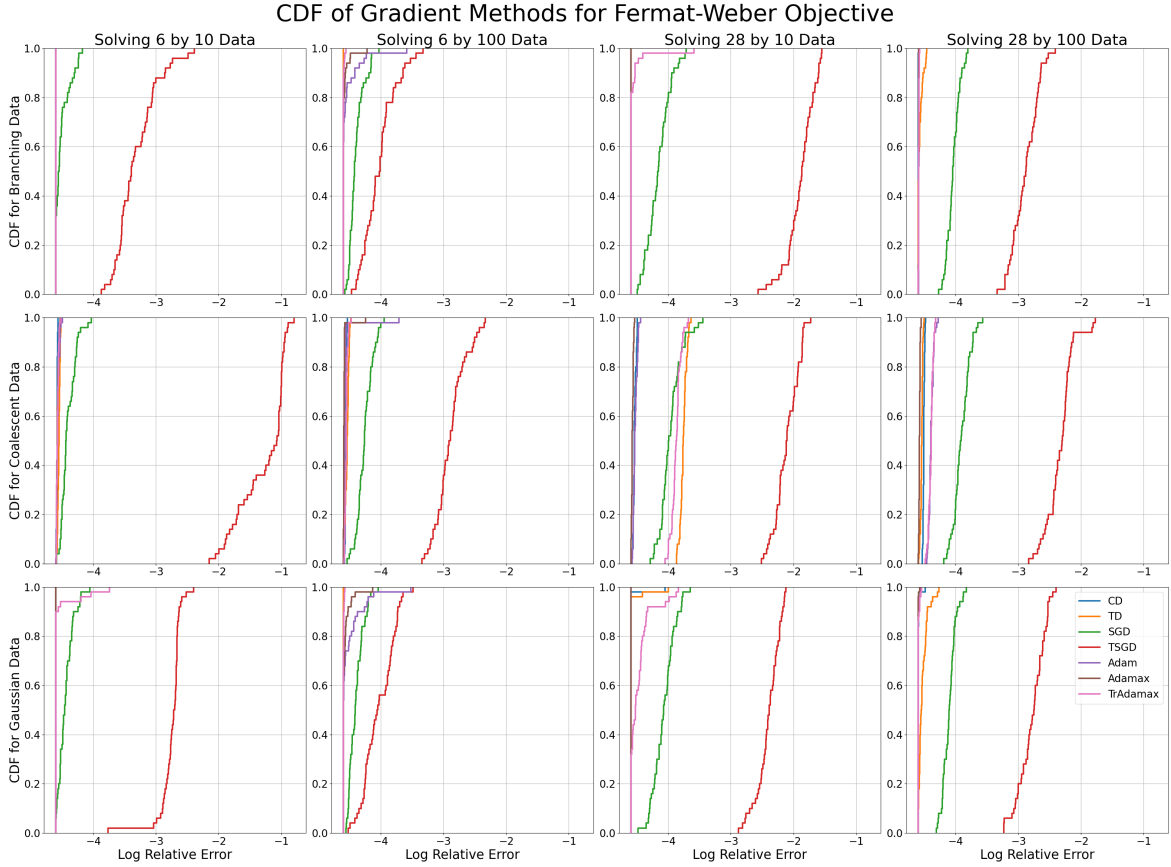


Figure 6: The CDF of the log relative error after 1000 steps for each gradient method with tuned learning rates across 50 random (Gaussian) initializations when minimizing the Fermat–Weber objective. Each subfigure corresponds to a dataset with sample size $K = 10, 100$ of dimensionality $N = 6, 28$, sampled from a branching process, coalescent process, or a Gaussian distribution.

Table 1: The mean log relative error of each gradient method after 1000 steps with tuned learning rates for branching process, coalescent process, and Gaussian datasets of size $K = 10, 100$ in $\mathbb{R}^6/\mathbb{R}\mathbf{1}$, $\mathbb{R}^{28}/\mathbb{R}\mathbf{1}$ when minimizing the Fermat–Weber objective function. The minimal mean errors for each dataset are in bold.

Data	CD	TD	SGD	TSGD	Adam	Adamax	TrAdamax
6×10 Branching Data	-4.60	-4.60	-4.50	-3.32	-4.60	-4.60	-4.60
6×10 Coalescent Data	-4.58	-4.55	-4.40	-1.28	-4.57	-4.57	-4.57
6×10 Gaussian Data	-4.60	-4.60	-4.44	-2.75	-4.60	-4.60	-4.56
6×100 Branching Data	-4.60	-4.60	-4.39	-4.02	-4.54	-4.58	-4.59
6×100 Coalescent Data	-4.55	-4.54	-4.25	-2.88	-4.56	-4.58	-4.55
6×100 Gaussian Data	-4.60	-4.60	-4.39	-4.03	-4.52	-4.57	-4.59
28×10 Branching Data	-4.60	-4.60	-4.15	-1.89	-4.60	-4.60	-4.56
28×10 Coalescent Data	-4.53	-3.76	-3.96	-2.11	-4.52	-4.57	-3.87
28×10 Gaussian Data	-4.58	-4.58	-4.07	-2.40	-4.60	-4.60	-4.47
28×100 Branching Data	-4.59	-4.57	-4.04	-2.89	-4.59	-4.59	-4.59
28×100 Coalescent Data	-4.51	-4.54	-3.91	-2.33	-4.39	-4.58	-4.39
28×100 Gaussian Data	-4.59	-4.53	-4.10	-2.78	-4.59	-4.59	-4.59

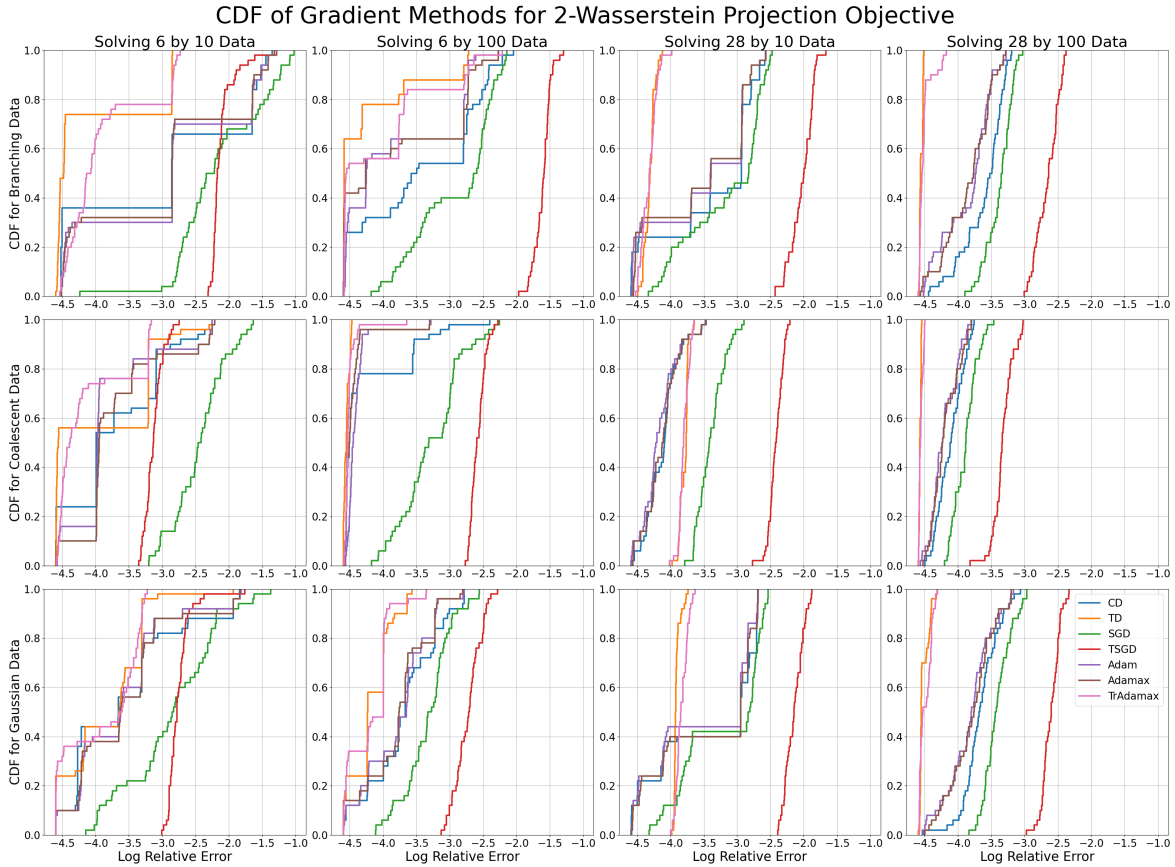


Figure 7: The CDF of the log relative error after 1000 steps for each gradient method with tuned learning rates across 50 random (Gaussian) initializations when minimizing the 2-Wasserstein projection objective. Each subfigure corresponds to a dataset with sample size $K = 10, 100$ of dimensionality $N = 6, 28$, sampled from a branching process, coalescent process, or a Gaussian distribution.

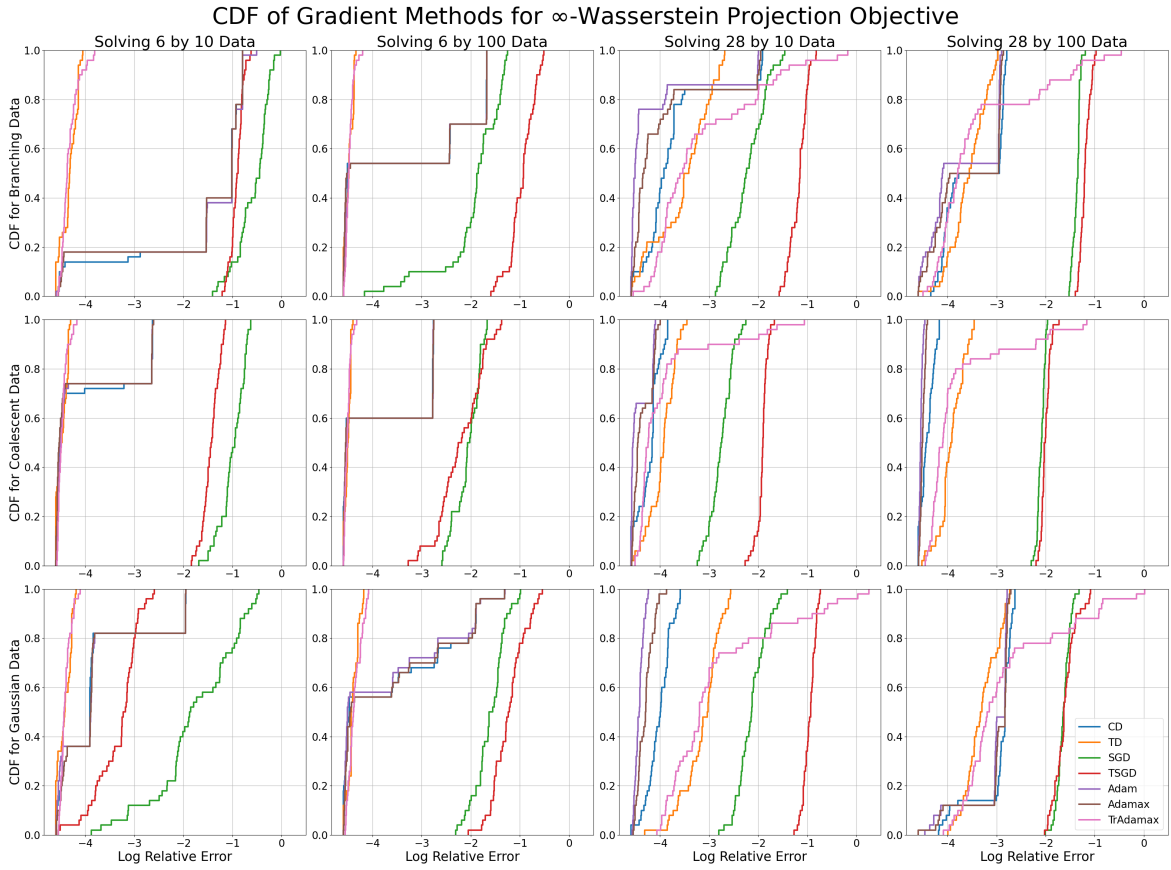


Figure 8: The CDF of the log relative error after 1000 steps for each gradient method with tuned learning rates across 50 random (Gaussian) initializations when minimizing the ∞ -Wasserstein projection objective. Each subfigure corresponds to a dataset with sample size $K = 10, 100$ of dimensionality $N = 6, 28$, sampled from a branching process, coalescent process, or a Gaussian distribution.

are particularly susceptible to this, while tropical descent and TrAdamax are more likely to pass these local minima. This difference is most pronounced when solving the ∞ -Wasserstein problem in low dimensions—we are almost certain to reach the minimum with relative error $\leq e^{-3}$, while classical methods have a 50-80% chance of achieving the same error.

4.2.3 Linear Regression

As the coalescent data lies on a tropical hyperplane (Ardila & Klivans, 2006; Page *et al.*, 2020), the minimum of the linear regression function for such data is exactly 0. Figure 9 therefore shows the CDF of the log error rather than the CDF of the log relative error.

Table 2: The mean log relative error of each gradient method after 1000 steps with tuned learning rates for branching process, coalescent process, and Gaussian datasets of size $K = 10, 100$ in $\mathbb{R}^6/\mathbb{R}\mathbf{1}$, $\mathbb{R}^{28}/\mathbb{R}\mathbf{1}$ when minimizing the linear regression objective function. The minimal mean errors for each dataset are in bold.

Data	CD	TD	SGD	TSGD	Adam	Adamax	TrAdamax
6×10 Branching Data	-0.97	-5.79	-0.56	-2.16	-0.80	-0.84	-4.39
6×10 Coalescent Data	-2.70	-5.87	-2.11	-5.47	-2.97	-2.66	-6.58
6×10 Gaussian Data	-1.19	-5.48	-0.80	-1.35	-1.05	-1.10	-4.10
6×100 Branching Data	-0.79	-5.49	-0.71	-1.43	-0.72	-0.72	-3.53
6×100 Coalescent Data	-5.54	-5.76	-3.11	-5.57	-6.90	-7.01	-6.52
6×100 Gaussian Data	-1.04	-5.50	-0.88	-1.70	-1.02	-1.02	-3.81
28×10 Branching Data	-1.49	-5.51	-0.93	-4.49	-1.14	-1.14	-5.57
28×10 Coalescent Data	-2.43	-6.63	-1.77	-5.55	-2.16	-2.29	-6.18
28×10 Gaussian Data	-1.26	-5.16	-0.79	-4.29	-1.08	-1.08	-5.72
28×100 Branching Data	-0.90	-4.37	-0.61	-1.42	-0.85	-0.77	-3.32
28×100 Coalescent Data	-3.33	-5.84	-2.17	-5.35	-3.02	-3.20	-4.93
28×100 Gaussian Data	-0.91	-4.35	-0.62	-1.07	-0.96	-0.90	-3.51

Table 2 shows the mean log errors of each gradient method and dataset, from which we see that the tropical methods outperform their classical counterparts for all but one dataset, often by a factor of two. In Figure 9 we see that the CDF of log errors for tropical descent and TrAdamax consistently dominates those of classical descent, Adam and Adamax, to the extent that the support of their CDFs does not intersect that of their classical counterparts for some datasets. We also note that unlike the previous problems, TSGD is outperforming SGD when solving the linear regression problem, often to the extent that TSGD outperforms all classical gradient methods.

4.3 Tropical Statistics for Applications

We conclude our computational experiments by using tropical gradient methods to solve tropical statistical problems which appear in phylogenetic data analysis and game theory. In particular we look to use tropical centrality statistics to estimate the species tree of a multi-species coalescent model (Liu *et al.*, 2019), and we use tropical linear regression to estimate the hidden preference factors in the Auction model introduced by Akian *et al.* (2023), which is a variant of the first-price sealed-bid auction model (Krishna, 2009).

4.3.1 Multi-species Coalescent Model

A *species tree* refers to a rooted metric tree which represents the evolutionary relationships between a set of species. However, for a specific gene, we may not observe the same branching pattern, instead observing a gene-specific evolution which is referred to as a *gene tree*. This raises one of the key questions in phylogenetics; how do we estimate the species tree from a set of gene trees? The multi-species coalescent model is a probabilistic model for gene trees given a certain species tree (see Liu *et al.* (2019) for a detailed introduction), which is particularly valuable for formulating Bayesian estimators for species trees and producing simulated data with which to test species tree estimation methodologies.

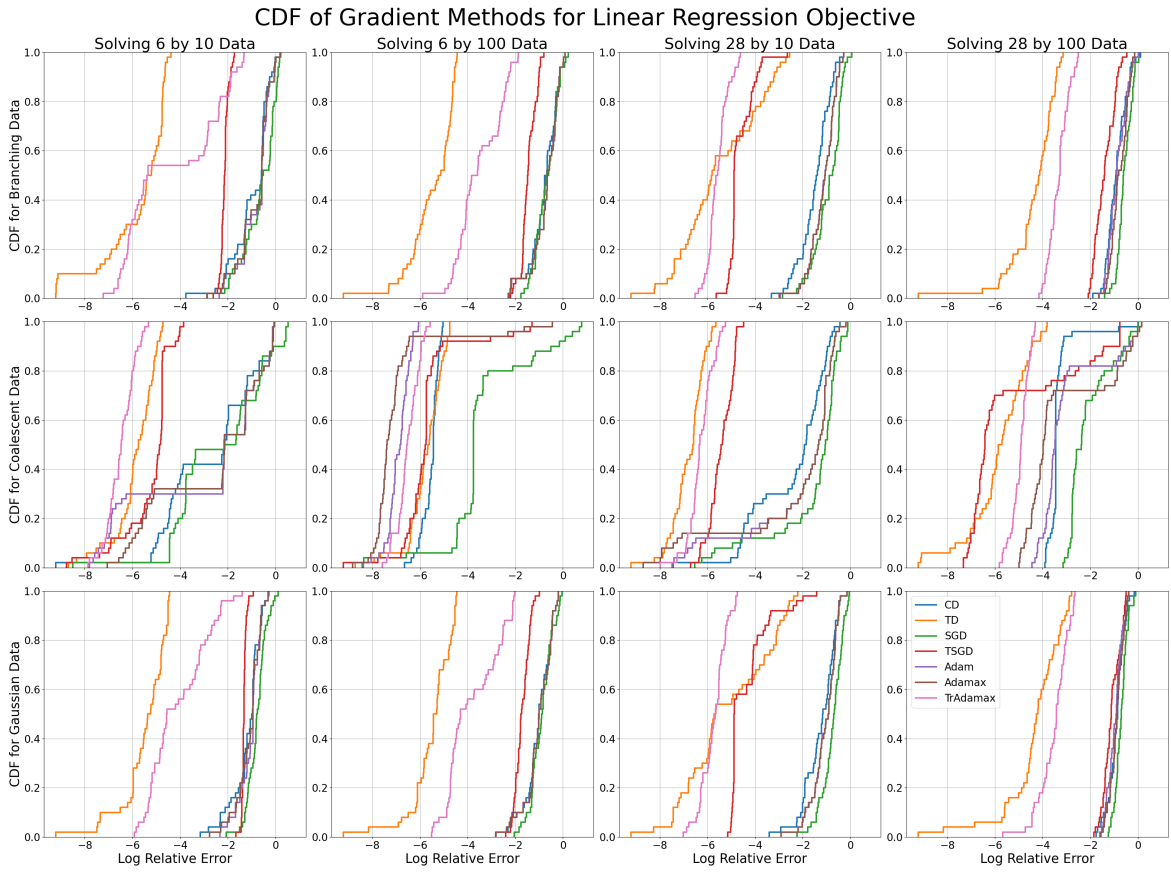


Figure 9: The CDF of the log error after 1000 steps for each gradient method with tuned learning rates across 50 random (Gaussian) initializations when minimizing the linear regression objective. Each subfigure corresponds to a dataset with sample size $K = 10, 100$ of dimensionality $N = 6, 28$, sampled from a branching process, coalescent process, or a Gaussian distribution.

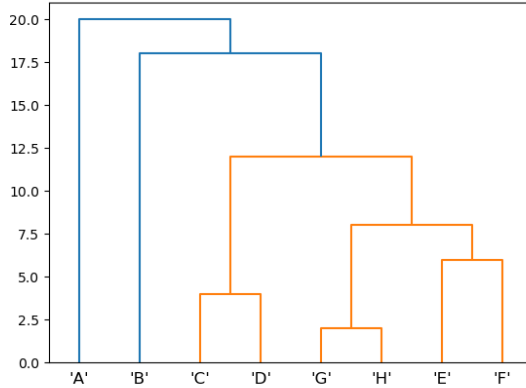


Figure 10: The underlying species tree used for the multi-species coalescent model generating our dataset of gene trees. The topology of this tree can be represented by the Newick string “((((F,E),(H,G)),(D,C)),B),A”.

Newick Tree	Adam	Adamax	CD	SGD	TD	TrAdamax	TSGD
((B,A),(((F,E),(H,G)),(D,C)));	0	0	0	0	0	0	2
0	0	0	3	0	0	0	
100	100	100	97	100	100	98	

Table 3: The counts of each Newick string (up to tree topology) returned by the tropical projection of a Fermat–Weber point computed via each gradient method. Each method is run for 1000 steps with trained learning rate, from 100 random initializations.

In this section, we consider the tropical Fermat-Weber and Fréchet means of gene trees as estimators for the underlying species tree. We fix a species tree with 8 leaves (see Figure 10), then use Dendropy (Moreno *et al.*, 2024) to sample 100 gene trees from a multi-species coalescent model with this underlying species tree and normalize this dataset to have average tropical norm 1.

We then compute a Fermat-Weber point and Fréchet mean for this dataset using each of our gradient methods for 1000 steps with their trained learning rates (Appendix C). We perform these computations from 100 random initializations for each gradient method, then project the result to ultrametric space using the single-linkage algorithm, which is known to coincide with tropical projection (Carlsson & Mémoli, 2010; Ardila, 2005), and record the topology of the resulting tree. The counts for each observed tree topology are presented in Tables 3 and 4.

We first note that in the vast majority of cases, our calculations recover the tree topology of the original species tree, suggesting that for this multi-species coalescent dataset, the tropical Fermat–Weber and Fréchet mean points are sufficiently good estimators for the species tree. When comparing the performance of each gradient method, we notice that the stochastic methods are the only methods to not recover the species tree topology, with Fréchet means computed via TSGD producing the highest error rate.

Newick Tree	Adam	Adamax	CD	SGD	TD	TrAdamax	TSGD
((B,A),(((F,E),(H,G)),(D,C)));	0	0	0	0	0	0	5
0	0	0	1	0	0	1	
100	100	100	99	100	100	94	

Table 4: The counts of each Newick string (up to tree topology) returned by the tropical projection of a Fréchet means computed via each gradient method. Each method is run for 1000 steps with trained learning rate, from 100 random initializations.

	K=6	K=100
Adam	(0.76 ± 0.33, 0.70 ± 0.32, 0.56 ± 0.21)	(0.77 ± 0.33, 0.71 ± 0.32, 0.58 ± 0.21)
Adamax	(0.76 ± 0.33, 0.70 ± 0.32, 0.56 ± 0.21)	(0.77 ± 0.33, 0.71 ± 0.32, 0.59 ± 0.21)
CD	(0.71 ± 0.43, 0.60 ± 0.42, 0.45 ± 0.30)	(0.78 ± 0.33, 0.70 ± 0.32, 0.58 ± 0.20)
SGD	(0.73 ± 0.44, 0.57 ± 0.43, 0.41 ± 0.32)	(0.77 ± 0.33, 0.70 ± 0.32, 0.58 ± 0.21)
TD	(1.00 ± 0.00, 0.81 ± 0.02, 0.60 ± 0.01)	(1.00 ± 0.02, 0.75 ± 0.08, 0.62 ± 0.05)
TrAdamax	(1.00 ± 0.00, 0.81 ± 0.00, 0.60 ± 0.00)	(0.93 ± 0.19, 0.79 ± 0.16, 0.65 ± 0.08)
TSGD	(1.00 ± 0.00, 0.82 ± 0.02, 0.60 ± 0.01)	(1.00 ± 0.04, 0.79 ± 0.04, 0.61 ± 0.01)

Table 5: The mean(± 1 std.) estimators $\hat{f} := \exp(\mathbf{t}_{1000} - \max(\mathbf{t}_{1000}))$ for the hidden preference factors in the Auction model (Akian *et al.*, 2023) when computed using gradient methods to solve the tropical linear regression problem. The true hidden preference factors are $f = (1, 0.8, 0.6)$. Akian *et al.* (2023) uses the projective Krasnoselskii-Mann iteration to solve this tropical linear regression problem, which produced an estimate of $f^{\text{reg}} = (1, 0.81, 0.605)$ for the $K = 6$ toy dataset.

The relative performance of tropical Fermat–Weber and Fréchet mean points as estimators for multi-species coalescent species trees is currently an open topic of study (Cox *et al.*, 2025). In exploring the consistency of these estimators it would be natural for future work to also consider the relative performance of tropical gradient methods for their computation.

4.3.2 Auction Model with Hidden Preference Factors

As a final computational demonstration, we use tropical gradient methods to solve the problem of tropical linear regression using the toy auction data example given by Akian *et al.* (2023). For N firms and K products, we let $(p_{ij})_{i \leq N, j \leq K}$ denote the price firm i offers for product j . Assuming the offered prices are in a state of equilibrium, that is, no firm can raise their price and still win, differences in proposed price from one firm relative to another is indicative of a hidden preference factor f_i in the market; that is, two firms’ offers for product j are considered equal when $p_{i_1j}f_{i_1} = p_{i_2j}f_{i_2}$. By performing tropical linear regression on the data $V_{ij} = \exp(-p_{ij})$, we can detect these hidden preference factors. For further details of this model and its assumptions, see Akian *et al.* (2023).

For our computations, we take $N = 3$ and $K = 6, 100$, using the same toy datasets discussed in Section 7.2 of Akian *et al.* (2023), which have true hidden preference factors $f = (1, 0.8, 0.6)$. We then perform each gradient method for 1000 steps over 100 random initializations, using learning rates which have been tuned to these datasets (Appendix C). Our estimates for f are then given by $\hat{f} := \exp(\mathbf{t}_{1000} - \max(\mathbf{t}_{1000}))$, such that $\max_i \hat{f}_i = 1$.

Table 5 shows the resulting mean estimates for these hidden preference factors when using different gradient methods to solve the tropical linear regression problem. We see that the accuracy of the tropical gradient methods vastly exceeds each of the classical gradient methods, and that these gradient methods produce particularly consistent results for the small sample problem.

These computations are limited to a single Auction model, but show promising results. For future work, it would be of interest to explore how the precision of these methods changes with sample size and dimension, as well as a running time comparison with existing methods such as the projective Krasnoselskii-Mann iteration used by Akian *et al.* (2023) or combinatorial simplex algorithms (Allamigeon *et al.*, 2014).

5 Conclusion and Discussion

We have introduced the concept of tropical descent as the steepest descent method with respect to the tropical norm. We have demonstrated, both theoretically and experimentally, that it exhibits desirable properties with respect to a wide class of optimization problems on the tropical projective torus, including several key statistical problems for the analysis of phylogenetic data. As well as proposing our own framework for tropical gradient methods, this work also provides a detailed review of the varying behavior of popular gradient methods when applied to tropical statistical optimization problems.

Our theoretical results outline the relative strengths of tropical descent over classical descent for tropical location problems, but only provide global solvability for 1-sample problems. In practice, our experimental

results go much further; the optimization problems studied are location problems, rather than Δ_{\min} -star-quasi-convex problems, and yet tropical descent appears to consistently converge to a global minimum, not just the tropical convex hull of our dataset. It would therefore be a natural extension of this work to identify how much we can relax the Δ_{\min} -star-quasi-convexity condition while guaranteeing global solvability.

In this paper we have considered tree data with 4 to 8 leaves, and samples of size 10 to 100—at this scale, we have observed (T/)SGD to be a significant sacrifice in accuracy with little benefit in computational time. Furthermore, at this scale, the relative merits of SGD versus its tropical counterpart are inconsistent; TSGD out-performs SGD when solving the linear regression problem, but performs worse when finding centrality statistics. In a similar vein, initial investigations suggest that the classical stochastic algorithm for the computation of Fréchet means—Sturm’s algorithm (Sturm *et al.*, 2003)—performs poorly for the computation of tropical Fréchet means due to the inconsistent curvature of the tropical projective torus (Amndola & Monod, 2023). However, for applications to larger datasets and more complex objective functions, stochastic gradient methods may become necessary. It would then be important to understand the theoretical differences between SGD and TSGD in terms of their convergence guarantees in the tropical setting and their comparative performance at different scales of data dimension.

The recent identification of tropical rational functions and ReLU neural networks (Zhang *et al.*, 2018) has inspired new avenues of research in tropical applications, such as the tropical geometry of neural networks (Brandenburg *et al.*, 2024; Yoshida *et al.*, 2024). It is therefore natural to consider the possible extensions of this work to neural network training; can we identify local tropical quasi-convexity in the loss functions of ReLU neural networks, and how can we extend tropical descent to the space of tropical rational functions?

Finally, as shown by Akian *et al.* (2023), the tropical linear regression problem is polynomial-time equivalent to mean payoff games—two-player perfect information games on a directed graph (Ehrenfeucht & Mycielski, 1979; Gurvich *et al.*, 1988). This family of problems is of particular interest in game theory as they are known to be $\text{NP} \cap \text{co-NP}$. In our numerical experiments, tropical gradient methods demonstrate a particularly strong performance in solving tropical linear regression, and while our methods are designed to approximate the minimum rather than compute it exactly, tropical descent may prove to be an efficient tool when solving large-scale mean payoff games.

Acknowledgements R.T. receives partial funding from a Technical University of Munich–Imperial College London Joint Academy of Doctoral Studies (JADS) award (2021 cohort, PIs Drton/Monod). A.M. is supported by EPSRC AI Hub on Mathematical Foundations of Intelligence: An “Erlangen Programme” for AI No. EP/Y028872/1.

Declarations

The authors have no relevant financial or non-financial interests to disclose. The authors have no competing interests to declare that are relevant to the content of this article. All authors certify that they have no affiliations with or involvement in any organization or entity with any financial interest or non-financial interest in the subject matter or materials discussed in this manuscript. The authors have no financial or proprietary interests in any material discussed in this article.

A PCA and Logistic Regression

As well as the location problems outlined in this paper, we performed the same numerical experiments with the tropical polytope PCA loss function (Yoshida *et al.*, 2019) and tropical logistic regression loss function (Aliatimis *et al.*, 2024). These loss functions take multiple points in $\mathbb{R}^N/\mathbb{R}\mathbf{1}$ as argument, and we execute our gradient methods on each argument simultaneously. Figures 11 and 12 show the resulting CDF of our gradient methods for these problems. These problems do not lend themselves well to gradient methods, as the relative log error is rather large for all of our proposed methods. However, for both problems the tropical descent and TrAdamax methods are outperforming the classical methods quite consistently.

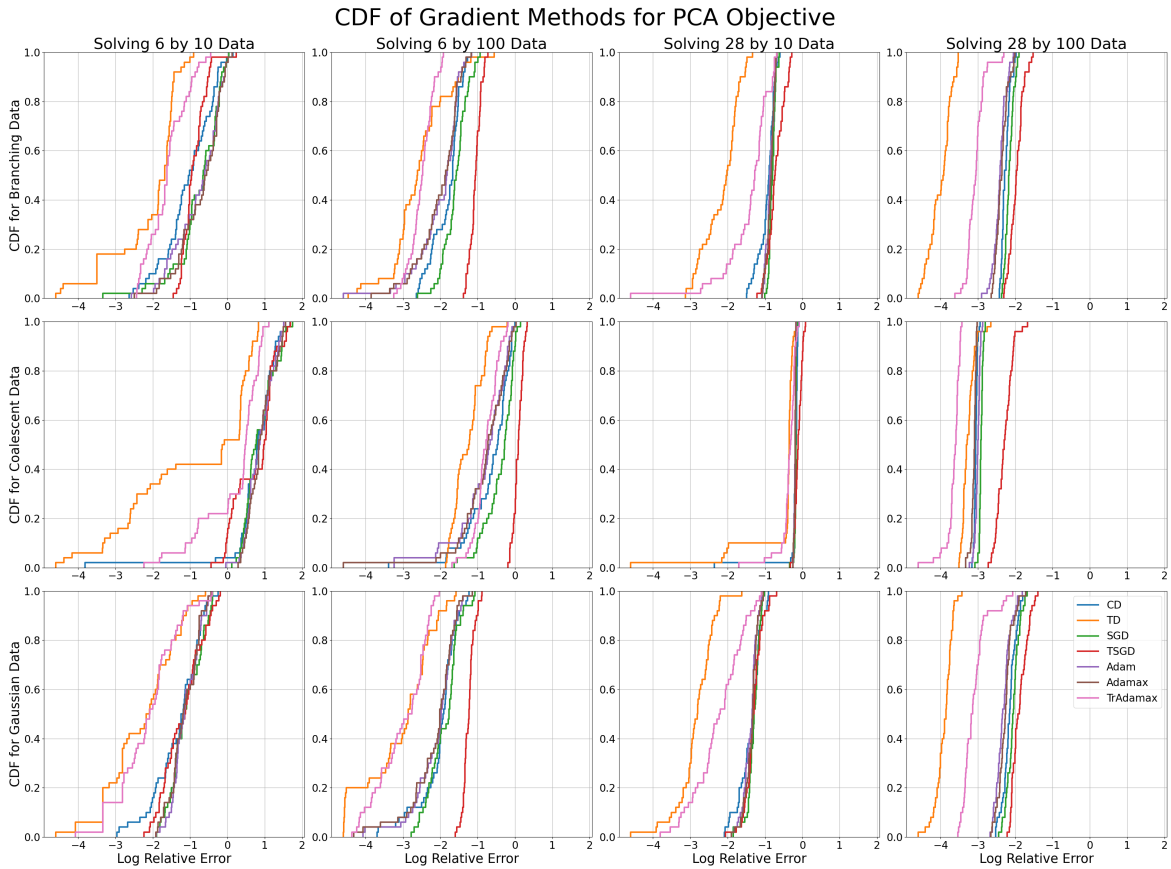


Figure 11: The CDF of the log relative error after 1000 steps for each gradient method with tuned learning rates across 50 random (Gaussian) initializations when minimizing the PCA objective. Each subfigure corresponds to a dataset with sample size $K = 10, 100$ of dimensionality $N = 6, 28$, sampled from a branching process, coalescent process, or a Gaussian distribution.

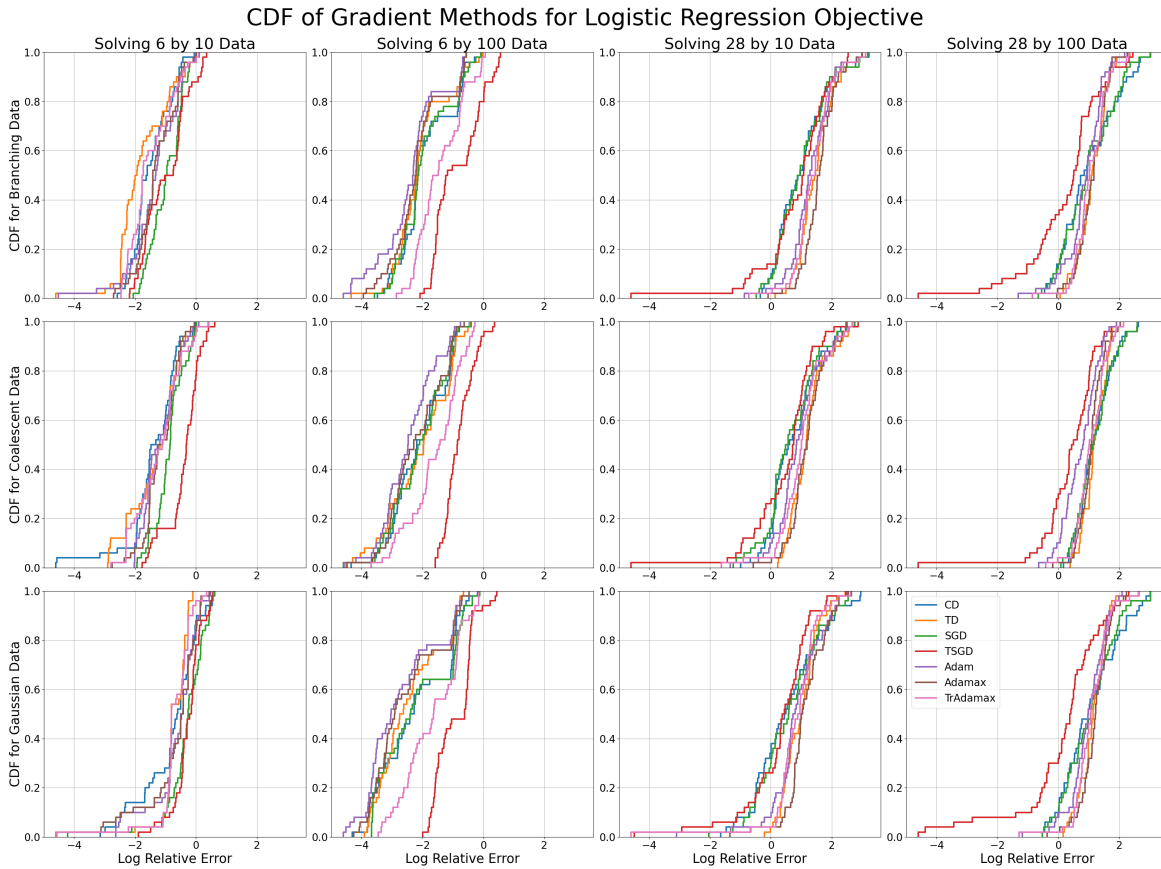


Figure 12: The CDF of the log relative error after 1000 steps for each gradient method with tuned learning rates across 50 random (Gaussian) initializations when minimizing the logistic regression objective. Each subfigure corresponds to a dataset with sample size $K = 10, 100$ of dimensionality $N = 6, 28$, sampled from a branching process, coalescent process, or a Gaussian distribution.

B Methodology

The same 12 datasets are used for each experiment in [Subsection 3.2](#) and [Section 4](#). These datasets live in $\mathbb{R}^6/\mathbb{R}\mathbf{1}$ or $\mathbb{R}^{28}/\mathbb{R}\mathbf{1}$; these dimensions correspond to the spaces of trees with 4 and 8 leaves respectively. Branching process datasets are generated using the R package `ape` (Paradis & Schliep, 2019) with exponentially distributed branch lengths—this produces data supported on the space of metric trees, i.e., the tropical Grassmannian. Coalescent data has also been generated using `ape` and is supported on the space of ultrametric trees, which is a tropical linear space. Gaussian data is generated using NumPy (Harris *et al.*, 2020), and is supported on the general tropical projective torus.

In the computation of the Wasserstein projection objectives, we require a secondary dataset of different dimensionality; for each of the 12 datasets, we generate datasets of the same size and distribution, but in $\mathbb{R}^3/\mathbb{R}\mathbf{1}$ or $\mathbb{R}^{21}/\mathbb{R}\mathbf{1}$ which contain the spaces of trees with 3 and 7 leaves respectively.

We use PyTorch (Paszke *et al.*, 2019) for the computation and differentiation of each objective function. Max-tropical descent directions are used for tropical gradient methods; we therefore optimize the min-tropical location problems—Wasserstein projections and tropical linear regression—with respect to $-\mathbf{t}$.

C Learning Rate Tuning

The Adam algorithms—Adam, Adamax and TrAdamax—are run using the default $\beta = (0.9, 0.999)$ parameters. We then tune the learning rates used for each method; CD, TD, SGD, TSGD, Adam, Adamax, and TrAdamax. We take 10 initializations at unit intervals on a log scale in the region $[e^{-6}, e^4]$ for each problem, gradient method, and data dimensionality. We then selected the learning rate with minimal mean log relative error in each case; [Tables 6 to 12](#) show the selected learning rates.

For the Auction data in [Subsection 4.3.2](#), we take 10 initializations at unit intervals in the region of $[e^{-10}, e^5]$ for each dataset; [Table 13](#) shows the selected learning rates which minimize the mean log relative error.

Table 6: Tuned learning rates for each gradient method when solving the Fermat–Weber problem.

Data Dim	Data Count	CD	TD	SGD	TSGD	Adam	Adamax	TrAdamax
6	10	0.135	0.135	0.135	0.135	0.00674	0.00674	0.00674
	100	0.135	0.135	0.135	0.135	0.00248	0.00248	0.00674
28	10	0.368	0.368	0.368	1	0.00674	0.00674	0.0183
	100	0.368	0.135	0.368	1	0.00674	0.00674	0.0183

Table 7: Tuned learning rates for each gradient method when solving the Fréchet mean problem.

Data Dim	Data Count	CD	TD	SGD	TSGD	Adam	Adamax	TrAdamax
6	10	0.135	0.135	0.135	0.135	0.00674	0.00674	0.00674
	100	0.135	0.135	0.135	0.135	0.00674	0.00248	0.00674
28	10	0.368	0.368	0.368	1	0.00674	0.00674	0.0183
	100	0.368	0.135	0.368	1	0.00674	0.00674	0.0183

D Run Times

Experiments were implemented on a AMD EPYC 7742 node using a single core, 96 GB. [Table 14](#) shows the average time taken per initialization for each gradient method and optimization problem.

Table 8: Tuned learning rates for each gradient method when solving the 2-Wasserstein projection problem.

Data Dim	Data Count	CD	TD	SGD	TSGD	Adam	Adamax	TrAdamax
6	10	2.72	1	1	0.135	0.135	0.368	0.368
	100	2.72	2.72	0.368	0.135	0.135	0.135	0.135
28	10	0.368	0.368	0.368	1	0.00674	0.0183	0.0183
	100	2.72	2.72	0.368	1	0.0498	0.135	0.0498

Table 9: Tuned learning rates for each gradient method when solving the ∞ -Wasserstein projection problem.

Data Dim	Data Count	CD	TD	SGD	TSGD	Adam	Adamax	TrAdamax
6	10	0.0498	0.135	0.0498	0.368	0.00674	0.00674	0.0183
	100	0.0498	0.135	0.135	2.72	0.00674	0.00674	0.0183
28	10	0.368	1	0.368	1	0.00674	0.0183	0.0498
	100	0.368	1	0.368	1	0.00674	0.0183	0.0498

Table 10: Tuned learning rates for each gradient method when solving the polytope PCA problem.

Data Dim	Data Count	CD	TD	SGD	TSGD	Adam	Adamax	TrAdamax
6	10	2.72	2.72	1	1	0.135	0.135	0.368
	100	2.72	7.39	1	1	0.135	0.135	1
28	10	7.39	7.39	0.368	1	0.0183	0.0183	0.135
	100	2.72	7.39	0.368	1	0.0498	0.0498	0.0498

Table 11: Tuned learning rates for each gradient method when solving the logistic regression problem.

Data Dim	Data Count	CD	TD	SGD	TSGD	Adam	Adamax	TrAdamax
6	10	7.39	2.72	1	2.72	0.368	1	0.0498
	100	1	0.368	1	2.72	0.00248	0.00248	0.00248
28	10	1	0.368	1	2.72	0.00248	0.00248	0.00674
	100	1	0.368	1	7.39	0.00248	0.00248	0.00674

Table 12: Tuned learning rates for each gradient method when solving the linear regression problem.

Data Dim	Data Count	CD	TD	SGD	TSGD	Adam	Adamax	TrAdamax
6	10	0.368	0.135	0.368	0.135	0.00248	0.0183	0.00674
	100	0.135	0.135	0.368	0.0498	0.00248	0.00248	0.00674
28	10	0.368	0.0498	0.0498	0.135	0.00248	0.00248	0.0183
	100	1	0.368	1	7.39	0.0498	0.0498	0.0498

Table 13: Tuned learning rates for each gradient method when solving the linear regression problem with Auction data.

Data Dim	Data Count	CD	TD	SGD	TSGD	Adam	Adamax	TrAdamax
3	6	2.72	0.368	7.39	0.0498	0.000912	0.000912	0.0183
	100	0.0183	2.72	0.0183	0.0498	0.000912	0.000912	0.00248

Table 14: Average run times for 1000 steps of each gradient method when minimizing each objective function.

Stats Prob	CD	TD	SGD	TSGD	Adam	Adamax	TrAdamax
Fermat–Weber	0.480	0.520	0.435	0.499	0.391	0.460	0.464
Fréchet Mean	0.347	0.363	0.301	0.342	0.294	0.422	0.370
2-Wasserstein Projection	2.739	2.134	2.392	2.209	2.341	2.246	2.272
∞ -Wasserstein Projection	2.947	3.049	2.772	2.565	2.501	3.162	2.807
Polytope PCA	1.117	1.081	1.014	1.052	1.037	1.174	1.029
Logistic Regression	0.987	1.015	0.962	0.934	0.943	1.084	0.943
Linear Regression	0.494	0.499	0.386	0.420	0.386	0.537	0.433

E Further Figures

E.1 Fréchet Means

Here we include the results for experiments run for the computation of Fréchet means. (Table 15, Figure 13)

Table 15: The mean log relative error of each gradient method after 1000 steps with tuned learning rates for branching process, coalescent process, and Gaussian datasets of size $K = 10, 100$ in $\mathbb{R}^6/\mathbb{R}\mathbf{1}$, $\mathbb{R}^{28}/\mathbb{R}\mathbf{1}$ when minimizing the Fréchet mean objective function. The minimal mean errors for each dataset are in bold.

Data	CD	TD	SGD	TSGD	Adam	Adamax	TrAdamax
6×10 Branching Data	-4.59	-4.54	-3.98	-2.99	-4.58	-4.59	-4.53
6×10 Coalescent Data	-4.58	-4.47	-4.07	-1.82	-4.57	-4.58	-4.45
6×10 Gaussian Data	-4.59	-4.33	-4.09	-2.63	-4.58	-4.59	-4.35
6×100 Branching Data	-4.59	-4.59	-4.35	-4.03	-4.59	-4.58	-4.59
6×100 Coalescent Data	-4.57	-4.56	-4.36	-3.29	-4.55	-4.56	-4.57
6×100 Gaussian Data	-4.59	-4.60	-4.39	-4.12	-4.59	-4.58	-4.59
28×10 Branching Data	-4.58	-3.73	-3.78	-1.98	-4.55	-4.58	-3.83
28×10 Coalescent Data	-4.56	-3.67	-3.98	-2.46	-4.53	-4.57	-3.70
28×10 Gaussian Data	-4.55	-4.07	-3.91	-2.41	-4.55	-4.57	-4.04
28×100 Branching Data	-4.59	-4.58	-4.03	-2.98	-4.58	-4.59	-4.57
28×100 Coalescent Data	-4.54	-4.56	-4.08	-2.66	-4.47	-4.57	-4.46
28×100 Gaussian Data	-4.59	-4.56	-4.08	-2.78	-4.59	-4.59	-4.58

E.2 Wasserstein Projections

From Tables 16 and 17, we see that when solving the 2-Wasserstein projection problem, tropical methods are optimal in all cases other than 28×10 coalescent data. For the ∞ -Wasserstein projection problem in small dimensions, tropical descent outperforms other methods by some margin, while the comparative performances are less consistent for the ∞ -Wasserstein projection problem in high dimensions.

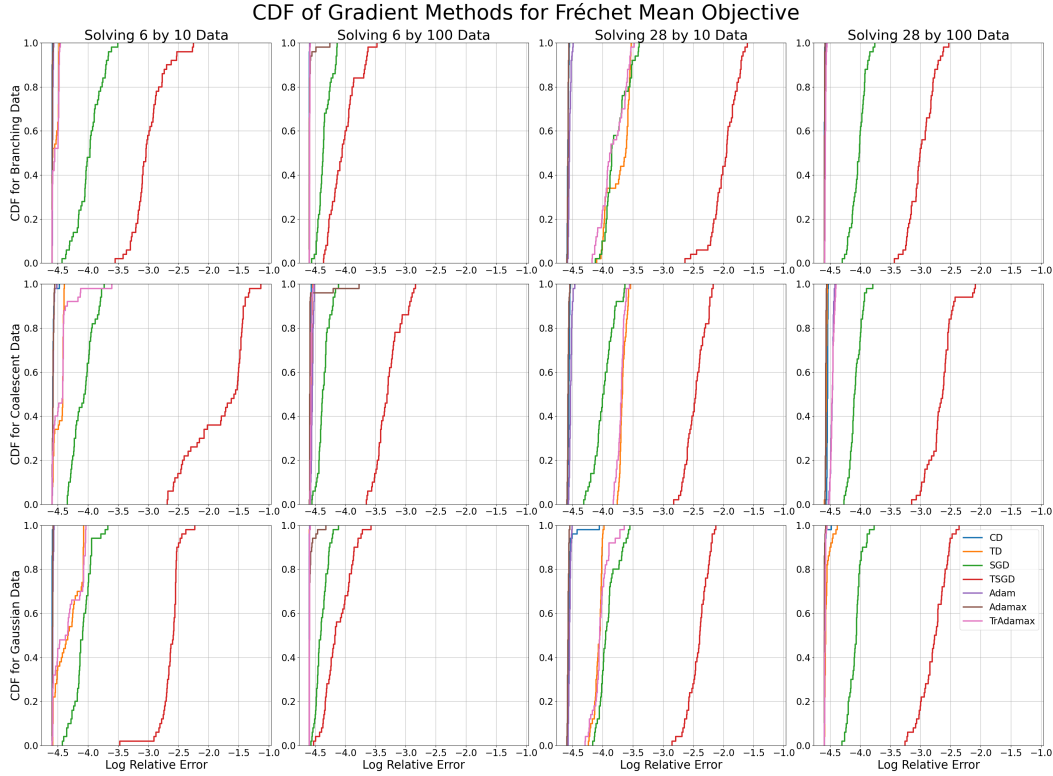


Figure 13: The CDF of the log relative error after 1000 steps for each gradient method with tuned learning rates across 50 random (Gaussian) initializations when minimizing the Fréchet mean objective. Each subfigure corresponds to a dataset with sample size $K = 10, 100$ of dimensionality $N = 6, 28$, sampled from a branching process, coalescent process, or a Gaussian distribution.

Table 16: The mean log relative error of each gradient method after 1000 steps with tuned learning rates for branching process, coalescent process, and Gaussian datasets of size $K = 10, 100$ in $\mathbb{R}^6/\mathbb{R}\mathbf{1}$, $\mathbb{R}^{28}/\mathbb{R}\mathbf{1}$ when minimizing the 2-Wasserstein projection objective function. The minimal mean errors for each dataset are in bold.

Data	CD	TD	SGD	TSGD	Adam	Adamax	TrAdamax
6×10 Branching Data	-3.02	-4.09	-2.16	-2.11	-2.95	-3.00	-3.89
6×10 Coalescent Data	-3.71	-3.92	-2.44	-3.13	-3.78	-3.68	-4.12
6×10 Gaussian Data	-3.59	-3.83	-2.87	-2.75	-3.61	-3.57	-3.89
6×100 Branching Data	-3.44	-4.24	-2.91	-1.60	-3.79	-3.79	-4.02
6×100 Coalescent Data	-4.26	-4.55	-3.27	-2.58	-4.39	-4.45	-4.50
6×100 Gaussian Data	-3.69	-4.17	-3.33	-2.73	-3.78	-3.78	-4.18
28×10 Branching Data	-3.39	-4.31	-3.16	-2.03	-3.53	-3.55	-4.32
28×10 Coalescent Data	-4.11	-3.79	-3.39	-2.42	-4.17	-4.12	-3.80
28×10 Gaussian Data	-3.43	-3.91	-3.21	-2.15	-3.50	-3.44	-3.83
28×100 Branching Data	-3.61	-4.55	-3.37	-2.65	-3.85	-3.85	-4.51
28×100 Coalescent Data	-4.11	-4.57	-3.89	-3.32	-4.21	-4.19	-4.56
28×100 Gaussian Data	-3.66	-4.52	-3.41	-2.61	-3.82	-3.80	-4.49

Table 17: The mean log relative error of each gradient method after 1000 steps with tuned learning rates for branching process, coalescent process, and Gaussian datasets of size $K = 10, 100$ in $\mathbb{R}^6/\mathbb{R}\mathbf{1}$, $\mathbb{R}^{28}/\mathbb{R}\mathbf{1}$ when minimizing the ∞ -Wasserstein projection objective function. The minimal mean errors for each dataset are in bold.

Data	CD	TD	SGD	TSGD	Adam	Adamax	TrAdamax
6×10 Branching Data	-1.63	-4.32	-0.57	-0.91	-1.68	-1.69	-4.32
6×10 Coalescent Data	-4.00	-4.47	-0.99	-1.43	-4.03	-4.04	-4.46
6×10 Gaussian Data	-3.77	-4.42	-1.76	-3.33	-3.76	-3.75	-4.40
6×100 Branching Data	-3.35	-4.48	-1.94	-0.95	-3.34	-3.36	-4.47
6×100 Coalescent Data	-3.85	-4.51	-2.06	-2.21	-3.84	-3.85	-4.51
6×100 Gaussian Data	-3.63	-4.40	-1.61	-1.22	-3.70	-3.63	-4.36
28×10 Branching Data	-3.68	-3.53	-2.22	-1.17	-4.11	-3.93	-3.17
28×10 Coalescent Data	-4.22	-3.95	-2.76	-1.92	-4.42	-4.36	-3.94
28×10 Gaussian Data	-4.02	-3.14	-2.13	-0.95	-4.43	-4.30	-2.85
28×100 Branching Data	-3.46	-3.58	-1.37	-1.19	-3.68	-3.59	-3.39
28×100 Coalescent Data	-4.41	-3.92	-2.09	-2.00	-4.54	-4.51	-3.81
28×100 Gaussian Data	-2.98	-3.30	-1.64	-1.61	-3.07	-3.04	-2.80

References

- AKIAN, MARIANNE, GAUBERT, STÉPHANE, QI, YANG, & SAADI, OMAR. 2023. Tropical Linear Regression and Mean Payoff Games: Or, How to Measure the Distance to Equilibria. *SIAM Journal on Discrete Mathematics*, **37**(2), 632–674.
- ALIATIMIS, GEORGIOS, YOSHIDA, RURIKO, BOYACI, BURAK, & GRANT, JAMES A. 2024. Tropical logistic regression model on space of phylogenetic trees. *Bulletin of Mathematical Biology*, **86**(8), 99.
- ALLAMIGEON, XAVIER, BENCHIMOL, PASCAL, GAUBERT, STÉPHANE, & JOSWIG, MICHAEL. 2014. Combinatorial simplex algorithms can solve mean payoff games. *SIAM Journal on Optimization*, **24**(4), 2096–2117.
- AMNDOLA, CARLOS, & MONOD, ANTHEA. 2023. An invitation to tropical Alexandrov curvature. *Algebraic Statistics*, **14**(2), 181214.
- ARDILA, FEDERICO. 2005. Subdominant matroid ultrametrics. *Annals of Combinatorics*, **8**, 379–389.
- ARDILA, FEDERICO, & KLIVANS, CAROLINE J. 2006. The Bergman complex of a matroid and phylogenetic trees. *Journal of Combinatorial Theory, Series B*, **96**(1), 38–49.
- BARNHILL, DAVID, YOSHIDA, RURIKO, ALIATIMIS, GEORGIOS, & MIURA, KEIJI. 2024. Tropical Geometric Tools for Machine Learning: the TML package. In: *2024 Joint Mathematics Meetings (JMM 2024)*. AMS.
- BILLERA, LOUIS J, HOLMES, SUSAN P, & VOGTMANN, KAREN. 2001. Geometry of the space of phylogenetic trees. *Advances in Applied Mathematics*, **27**(4), 733–767.
- BOYD, STEPHEN, & VANDENBERGHE, LIEVEN. 2004. *Convex Optimization*. Cambridge: Cambridge University Press.
- BRANDENBURG, MARIE CHARLOTTE, LOHO, GEORG, & MONTÚFAR, GUIDO. 2024. The real tropical geometry of neural networks for binary classification. *Transactions on Machine Learning Research*.
- CAI, YUHANG, & LIM, LEK-HENG. 2022. Distances Between Probability Distributions of Different Dimensions. *IEEE Transactions on Information Theory*, **68**(6), 4020–4031.
- CARLSSON, GUNNAR, & MÉMOLI, FACUNDO. 2010. Characterization, Stability and Convergence of Hierarchical Clustering Methods. *Journal of Machine Learning Research*, **11**(47), 1425–1470.
- COMĂNECI, ANDREI. 2024. Tropical convexity in location problems. *Mathematical Methods of Operations Research*, 1–26.
- COMĂNECI, ANDREI, & JOSWIG, MICHAEL. 2024. Tropical medians by transportation. *Mathematical Programming*, **205**(1), 813–839.
- COX, SHELBY, SABOL, JOHN, TALBUT, ROAN, & YOSHIDA, RURIKO. 2025. Tropical Fermat-Weber Points over Bergman Fans. *arXiv preprint arXiv:2505.09584*.
- DEVELIN, MIKE, & STURMFELS, BERND. 2004. Tropical convexity. *Documenta Mathematica*, **9**, 1–27.
- DREZNER, ZVI, KLAMROTH, KATHERIN, SCHÖBEL, ANITA, & WESOLOWSKY, GEORGE O. 2004. The Weber problem. In: *Facility location: applications and theory*. Heidelberg: Springer Berlin.
- EHRENFEUCHT, ANDRZEJ, & MYCIELSKI, JAN. 1979. Positional strategies for mean payoff games. *International Journal of Game Theory*, **8**, 109–113.
- FRÉCHET, MAURICE. 1948. Les éléments aléatoires de nature quelconque dans un espace distancié. *Pages 215–310 of: Annales de l’institut Henri Poincaré*, vol. 10.
- GÄRTNER, BERND, & JAGGI, MARTIN. 2006. *Tropical support vector machines*. ACS Technical Report. No.: ACS-TR-362502-01.

- GURVICH, VA, KARZANOV, AV, & KHACHIYAN, LG. 1988. Cyclic games and finding minimax mean cycles in digraphs. *Zh. Vychisl. Mat. i Mat. Fiz.*, **28**(9), 1407–1417.
- HARRIS, CHARLES R., MILLMAN, K. JARROD, VAN DER WALT, STÉFAN J., GOMMERS, RALF, VIRTANEN, PAULI, COURNAPEAU, DAVID, WIESER, ERIC, TAYLOR, JULIAN, BERG, SEBASTIAN, SMITH, NATHANIEL J., KERN, ROBERT, PICUS, MATTI, HOYER, STEPHAN, VAN KERKWIJK, MARTEN H., BRETT, MATTHEW, HALDANE, ALLAN, DEL RÍO, JAIME FERNÁNDEZ, WIEBE, MARK, PETERSON, PEARU, GÉRARD-MARCHANT, PIERRE, SHEPPARD, KEVIN, REDDY, TYLER, WECKESSER, WARREN, ABBASI, HAMEER, GOHLKE, CHRISTOPH, & OLIPHANT, TRAVIS E. 2020. Array programming with NumPy. *Nature*, **585**(7825), 357–362.
- KAHN, SCOTT D. 2011. On the future of genomic data. *science*, **331**, 728–729.
- KINGMA, DIEDERIK, & BA, JIMMY. 2015. Adam: A Method for Stochastic Optimization. *In: International Conference on Learning Representations (ICLR)*.
- KIWIEL, KRZYSZTOF C. 1985. *Methods of Descent for Nondifferentiable Optimization*. Lecture Notes in Mathematics, vol. 1133. Berlin, Heidelberg: Springer.
- KRISHNA, VIJAY. 2009. *Auction theory*. 2nd ed. edn. Boston: Elsevier Academic Press.
- LAPORTE, GILBERT, NICKEL, STEFAN, & SALDANHA-DA GAMA, FRANCISCO. 2019. Introduction to Location Science. *Pages 1–21 of: Location Science*. Cham: Springer International Publishing.
- LEE, WONJUN, LI, WUCHEN, LIN, BO, & MONOD, ANTHEA. 2022. Tropical optimal transport and Wasserstein distances. *Information Geometry*, **5**(1), 247–287.
- LIN, BO, & TRAN, NGOC MAI. 2019. Two-player incentive compatible outcome functions are affine maximizers. *Linear Algebra and its Applications*, **578**, 133–152.
- LIN, BO, & YOSHIDA, RURIKO. 2018. Tropical Fermat–Weber Points. *SIAM Journal on Discrete Mathematics*, **32**(2), 1229–1245.
- LIU, LIANG, ANDERSON, CHRISTIAN, PEARL, DENNIS, & EDWARDS, SCOTT V. 2019. Modern phylogenomics: building phylogenetic trees using the multispecies coalescent model. *Pages 211–239 of: Evolutionary genomics: statistical and computational methods*. Humana, New York, NY: Springer.
- MACLAGAN, DIANE, & STURMFELS, BERND. 2015. *Introduction to Tropical Geometry*. Graduate Studies in Mathematics, vol. 161. Providence, RI: American Mathematical Society.
- MONOD, ANTHEA, LIN, BO, YOSHIDA, RURIKO, & KANG, QIWEN. 2018. Tropical geometry of phylogenetic tree space: a statistical perspective. *arXiv preprint arXiv:1805.12400*.
- MORENO, MATTHEW ANDRES, HOLDER, MARK T., & SUKUMARAN, JEET. 2024. *DendroPy 5: a mature Python library for phylogenetic computing*.
- PAGE, ROBERT, YOSHIDA, RURIKO, & ZHANG, LEON. 2020. Tropical principal component analysis on the space of phylogenetic trees. *Bioinformatics*, **36**(17), 4590–4598.
- PARADIS, EMMANUEL, & SCHLIEP, KLAUS. 2019. Ape 5.0: an environment for modern phylogenetics and evolutionary analyses in R. *Bioinformatics*, **35**(3), 526–528.
- PASQUE, KURT, TESKA, CHRISTOPHER, YOSHIDA, RURIKO, MIURA, KEIJI, & HUANG, JEFFERSON. 2024. Tropical decision boundaries for neural networks are robust against adversarial attacks. *arXiv preprint arXiv:2402.00576*.
- PASZKE, ADAM, GROSS, SAM, MASSA, FRANCISCO, LERER, ADAM, BRADBURY, JAMES, CHANAN, GREGORY, KILLEEN, TREVOR, LIN, ZEMING, GIMELSHEIN, NATALIA, ANTIGA, LUCA, DESMAISON, ALBAN, KOPF, ANDREAS, YANG, EDWARD, DEVITO, ZACHARY, RAISON, MARTIN, TEJANI, ALYKHAN, CHILAMKURTHY, SASANK, STEINER, BENOIT, FANG, LU, BAI, JUNJIE, & CHINTALA, SOUMITH. 2019. PyTorch: An Imperative Style, High-Performance Deep Learning Library. *Pages 8024–8035 of: Advances in Neural Information Processing Systems 32*. Vancouver, BC, Canada: Curran Associates, Inc.

- ROBINSON, D.F., & FOULDS, L.R. 1981. Comparison of phylogenetic trees. *Mathematical Biosciences*, **53**(1), 131–147.
- SABOL, JOHN, BARNHILL, DAVID, YOSHIDA, RURIKO, & MIURA, KEIJI. 2024. Tropical Fermat-Weber Polytopes. *arXiv preprint arXiv:2402.14287*.
- SPEYER, DAVID, & STURMFELS, BERND. 2004. The Tropical Grassmannian. *Adv. Geom.*, **4**(3), 389–411.
- STEEL, MIKE A., & PENNY, DAVID. 1993. Distributions of Tree Comparison Metrics—Some New Results. *Systematic Biology*, **42**(2), 126–141.
- STURM, KARL-THEODOR, COULHON, THIERRY, GRIGORYAN, ALEXANDER, & AUSCHER, PASCAL. 2003. Probability measures on metric spaces of nonpositive curvature. *Pages 357–390 of: Heat Kernels and Analysis on Manifolds, Graphs, and Metric Spaces*. Contemporary Mathematics, vol. 338. Providence, Rhode Island: American Mathematical Society.
- TALBUT, ROAN, TRAMONTANO, DANIELE, CAO, YUEQI, DRTON, MATHIAS, & MONOD, ANTHEA. 2023. Probability Metrics for Tropical Spaces of Different Dimensions. *arXiv preprint arXiv:2307.02846*.
- TANG, XIAOXIAN, WANG, HOUIE, & YOSHIDA, RURIKO. 2024. Tropical support vector machine and its applications to phylogenomics. *Algebraic Statistics*, **14**(2), 133–165.
- YOSHIDA, RURIKO. 2022. Tropical data science over the space of phylogenetic trees. *Pages 340–361 of: Intelligent Systems and Applications: Proceedings of the 2021 Intelligent Systems Conference (IntelliSys) Volume 2*. Springer.
- YOSHIDA, RURIKO, ZHANG, LEON, & ZHANG, XU. 2019. Tropical principal component analysis and its application to phylogenetics. *Bulletin of mathematical biology*, **81**(2), 568–597.
- YOSHIDA, RURIKO, TAKAMORI, MISAKI, MATSUMOTO, HIDEYUKI, & MIURA, KEIJI. 2023. Tropical support vector machines: Evaluations and extension to function spaces. *Neural Networks*, **157**, 77–89.
- YOSHIDA, RURIKO, ALIATIMIS, GEORGIOS, & MIURA, KEIJI. 2024. Tropical neural networks and its applications to classifying phylogenetic trees. *Pages 1–9 of: 2024 International Joint Conference on Neural Networks (IJCNN)*. IEEE.
- ZHANG, LIWEN, NAITZAT, GREGORY, & LIM, LEK-HENG. 2018. Tropical geometry of deep neural networks. *Pages 5824–5832 of: International Conference on Machine Learning*. PMLR.